Journal of Medicinal Chemistry

Article

pubs.acs.org/jmc

Structure-Based Discovery of 4-(6-Methoxy-2-methyl-4-(quinolin-4-yl)-9*H*-pyrimido[4,5-*b*]indol-7-yl)-3,5-dimethylisoxazole (CD161) as a Potent and Orally Bioavailable BET Bromodomain Inhibitor

Yujun Zhao,[†,∥] Longchuan Bai,[†] Liu Liu,[†] Donna McEachern,[†] Jeanne A. Stuckey,[§] Jennifer L. Meagher,[§] Chao-Yie Yang,[†] Xu Ran,[†,⊥] Bing Zhou,[†,∥] Yang Hu,[†] Xiaoqin Li,[‡] Bo Wen,[‡] Ting Zhao,[‡] Siwei Li,[‡] Duxin Sun,[‡] and Shaomeng Wang*[,†]

[†]Comprehensive Cancer Center and Departments of Internal Medicine, Pharmacology, and Medicinal Chemistry, University of Michigan, Ann Arbor, Michigan 48109, United States

[‡]Department of Pharmaceutical Sciences, College of Pharmacy, University of Michigan, Ann Arbor, Michigan 48109, United States

[§]Life Sciences Institute and Department of Biological Chemistry, University of Michigan, Ann Arbor, Michigan 48109, United States

Supporting Information

ABSTRACT: We have designed and synthesized 9*H*-pyrimido[4,5-*b*]indole-containing compounds to obtain potent and orally bioavailable BET inhibitors. By incorporation of an indole or a quinoline moiety to the 9*H*-pyrimido[4,5-*b*]indole core, we identified a series of small molecules showing high binding affinities to BET proteins and low nanomolar potencies in inhibition of cell growth in acute leukemia cell lines. One such compound, 4-(6-methoxy-2-methyl-4-(quinolin-4-yl)-9*H*-pyrimido[4,5-*b*]indol-7-yl)-3,5-dimethylisoxazole (**31**) has excellent microsomal stability and good oral pharmacokinetics in rats and mice. Orally administered, **31** achieves significant antitumor activity in the MV4;11 leukemia and MDA-MB-231 triple-negative breast cancer xenograft models in mice. Determination of the cocrystal structure of **31** with BRD4 BD2 provides a structural basis for its high binding affinity to BET proteins. Testing its binding affinities against other bromodomain-containing proteins shows that **31** is a highly selective inhibitor of BET proteins. Our data show that **31** is a potent, selective, and orally active BET inhibitor.

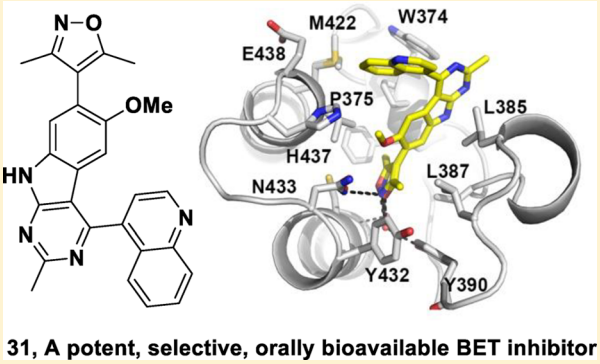

31, A potent, selective, orally bioavailable BET inhibitor

INTRODUCTION

Acetylation of lysine residues at the histone tail plays a central role in the dynamic regulation of chromatin-based gene transcription. Bromodomain-containing proteins (BRDs) function as epigenetic "readers" by binding to acetyl-lysine residues in the histone tail and regulate gene expression.[1,2] Bromodomain and extra-terminal (BET) proteins are one subfamily of BRDs which has four members, BRD2, BRD3, BRD4, and testis-specific BRDT. BET proteins have been implicated in a variety of human diseases, including NUT midline carcinoma,[3] MLL1-fusion leukemia,[4] inflammatory diseases,[5] and acute heart failure.[6]

Structurally, BET proteins consist of two tandem bromodomains (BD1 and BD2) both of which bind to acetyl-lysine (Ac-K) residues in the histone tails. Small molecule BET inhibitors, such as JQ-1 (**1**, Figure 1),[3] have been discovered that bind to the acetyl-lysine binding pocket in the BET proteins.[3,5,7−19] Potent and selective BET inhibitors are powerful tools with which to investigate the role of BET proteins in different biological and pathological processes.[3−6,18,20−27] In preclinical studies, BET inhibitors have demonstrated their therapeutic potential in the treatment of human cancers, inflammation, HIV infection, acute heart failure, and other disorders. Several BET inhibitors including OTX-015 (**2**),[18] CPI-0610 (**3**),[28] I-BET762 (**4**) (Figure 1) are currently being evaluated in human clinical trials for the treatment of different cancers. Recently obtained clinical data have provided an important proof of the concept that BET small-molecule inhibitors may have a therapeutic potential for the treatment of several forms of human cancer.[29−32]

Our laboratory previously reported the design of a new class of BET bromodomain inhibitors containing a tricyclic 5*H*-pyrido[4,3-*b*]indole structure, exemplified by RX-37 (**6**).[33] This compound binds to BET proteins with nanomolar affinities and demonstrates high selectivity over other bromodomain-containing proteins.[33] It potently inhibits cell growth in the MV4;11 and MOLM-13 acute leukemia cell lines harboring mixed lineage leukemia 1 (MLL1) fusion protein and has a high specificity for the K562 leukemia cell line harboring BCR-ABL

Received: February 4, 2017

DOI: 10.1021/acs.jmedchem.7b00193
J. Med. Chem. XXXX, XXX, XXX−XXX

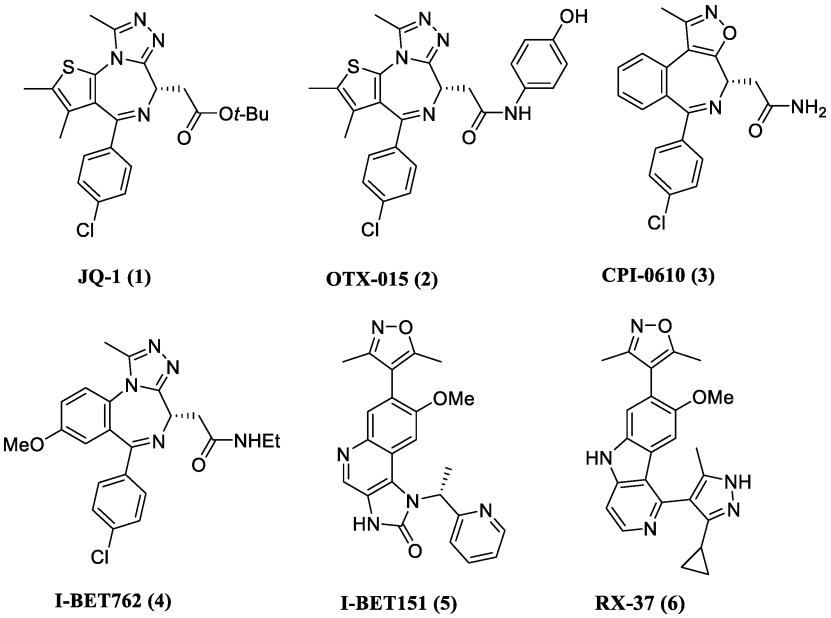

Figure 1. Representative, previously reported potent BET bromodomain inhibitors.

fusion protein.[33] Hence, **6** represents a promising lead compound for further optimization toward our goal of development of a new class of potent, selective, efficacious BET inhibitors for the treatment of human cancers and other medical conditions.

Our previously reported synthetic routes to **6** are not suited to large scale synthesis, and this has limited the exploration of its structure−activity relationships (SAR) and potential in vivo evaluation of this class of compounds. We have therefore decided to develop alternative tricyclic core structures, which allowed us to explore the SAR more extensively and comprehensively. In the present study, we report our efforts to obtain potent, efficacious, and orally active BET inhibitors. This has resulted in the discovery of compound **31**, which binds to BET proteins with high affinities and potently inhibits cell growth in acute leukemia cell lines harboring the MLL1 fusion protein and in a panel of human breast cancer cell lines. Significantly, compound **31** has an excellent oral pharmacokinetic profile and, orally administered, effectively inhibits tumor growth in mice.

RESULTS AND DISCUSSION

Analysis of the cocrystal structure of **6** in a complex with BRD4 BD2 protein shows that one additional nitrogen atom can be inserted into the 5*H*-pyrido[4,3-*b*]indole structure (Table 1) without causing any unfavorable interactions with the protein. This led to the design of compounds containing the 9*H*-pyrimido[4,5-*b*]indole core structure, which can be more efficiently synthesized than the core structure of **6** as shown in Schemes 1 and 2.

We first synthesized compound **7** to test this new core for the design of potent BET inhibitors. This compound binds to recombinant human BRD4 BD1 and BD2 proteins with K_i = 387 nM and 476 nM, respectively (Table 1), in our competitive fluorescence-polarization assays.[33] Since this compound still lacks a moiety to interact with the well-defined "WPF" hydrophobic pocket in the BRD4 protein, it therefore represents a reasonable starting point for further optimization.

Our previous SAR data of compound **6** and its analogues demonstrated that targeting the "WPF" hydrophobic pocket in BET proteins is a very effective way of improving the binding affinities of BET inhibitors.[33] Overlay of our modeled structure of **7** in a complex with BRD4 BD2 and the cocrystal structure[4] of compound **5** (I-BET151) complexed with BRD4 BD2 led to the design of **8** (Table 1), which contains the same hydrophobic group as was used in **5** to target the "WPF" hydrophobic pocket. Compound **8** binds to BRD4 BD1 and BD2 with K_i = 12.0 nM and 10.4 nM (Table 1) and is thus >30 times more potent than **7**, further supporting the precept that targeting the WPF binding pocket can indeed significantly improve the binding affinity of BET inhibitors. In comparison, compound **8** is as potent as **1** and **6** in binding to both BDR4 BD1 and BD2 proteins.

In our previous study, we found that substituted five-membered aromatic rings such as that in compound **6** can be used to effectively target the "WPF" pocket in BET proteins.[7,10−17,28,33] Accordingly, we next further explored the SAR resulting from targeting the "WPF" pocket using different five-membered aromatic rings (Table 2). Among compounds **9**−**13**, which contain an unsubstituted five-membered ring, compounds **11** and **12**

Table 1. Design of BET Inhibitors Containing a 9*H*-Pyrimido[4,5-*b*]indole Tricyclic Core Structure

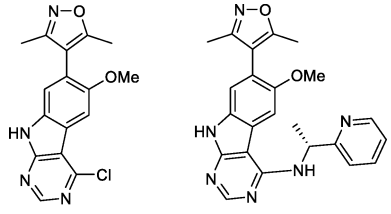

7 (CD55) **8** (CD57)

	BRD4 BD1		BRD4 BD2	
compd	IC_{50} (nM)	K_i (nM)	IC_{50} (nM)	K_i (nM)
1	46.7 ± 4.4	14.9 ± 2.6	42.2 ± 9.1	12.0 ± 3.5
4	145 ± 22	46.4 ± 6.4	77.5 ± 15.0	23.0 ± 4.2
5	31.7 ± 7.7	9.0 ± 2.9	226 ± 44	74.8 ± 8.6
6	75.5 ± 6.2	24.7 ± 1.0	36.5 ± 8.9	12.2 ± 1.6
7	1125 ± 92	387 ± 46	1760 ± 396	476 ± 86
8	39.2 ± 11.6	12.0 ± 3.5	26.4 ± 5.3	10.4 ± 1.1

DOI: 10.1021/acs.jmedchem.7b00193
J. Med. Chem. XXXX, XXX, XXX−XXX

Scheme 1. Synthesis of Key Intermediate 7[a]

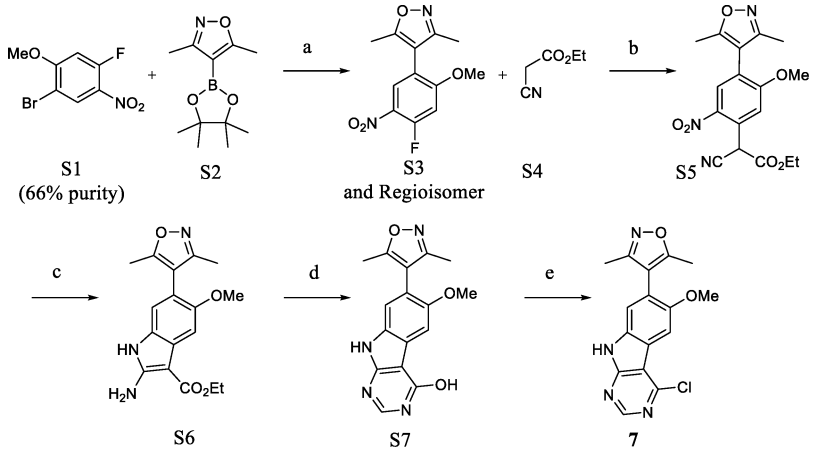

[a]Reaction conditions: (a) $Pd(PPh_3)_4$, DME−H_2O, reflux overnight, >80% yield; (b) NaH, anhydrous DMF, overnight, 53% yield; (c) Zn, HOAc, 85 °C, 3 h, 47% yield; (d) ammonium formate 2.0 equiv, formamide, 175 °C, 16 h, 55% yield; (e) $POCl_3$, 90 °C, 5 h, 66% yield.

Scheme 2. Synthesis of Common Intermediate, S10[a]

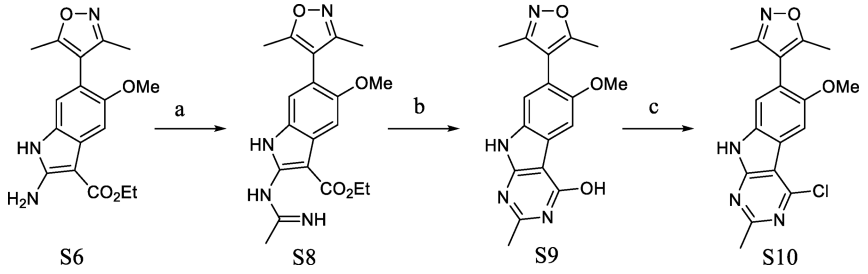

[a]Reaction conditions: (a) **S6** in dry MeCN, bubble HCl gas for 30 min, then reflux 2.5 h; (b) **S8** in EtOH, 10% NaOH aq, reflux 6 h, 78% over two steps; (b) $POCl_3$, 90 °C, 5 h, 75% yield.

Table 2. Design of BET Inhibitors Targeting the WPF Binding Pocket Using Five-Membered Aromatic Rings

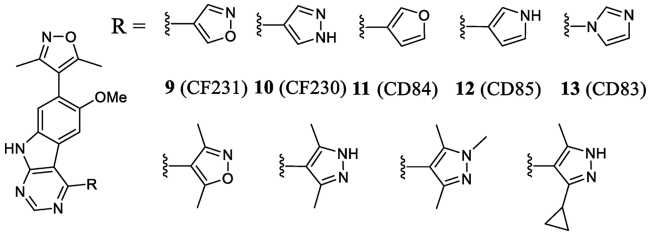

9 (CF231) **10** (CF230) **11** (CD84) **12** (CD85) **13** (CD83)

14 (CD58) **15** (CD64) **16**(CD63) **17** (CD133)

	BRD4 BD1		BRD4 BD2	
compd	IC_{50} (nM)	K_i (nM)	IC_{50} (nM)	K_i (nM)
9	2060 ± 420	655 ± 269	1882 ± 406	641 ± 200
10	393 ± 127	131 ± 50	199 ± 81	57.0 ± 17.3
11	155 ± 47	44.3 ± 13.9	180 ± 37	56.4 ± 11.7
12	165 ± 50	51.9 ± 18.6	108 ± 37	30.6 ± 9.0
13	1456 ± 441	456 ± 150	1139 ± 198	335 ± 25
14	102 ± 40	41.2 ± 16.9	164 ± 44	68.7 ± 21.4
15	51.7 ± 15.0	19.7 ± 8.2	63.5 ± 16.4	20.2 ± 9.2
16	40.9 ± 14.2	18.5 ± 4.0	89.7 ± 18.5	31.2 ± 11.8
17	24.1 ± 5.5	7.0 ± 3.3	11.7 ± 2.0	2.7 ± 0.5

containing a furan and a pyrrole respectively have the highest binding affinities and are both >5 times more potent than **7** in binding to both BRD4 BD1 and BD2 proteins.

In the cocrystal structure of compound **6** complexed with BRD4 BD2, the cyclopropyl group is inserted deeply into the WPF hydrophobic pocket,[33] suggesting that additional hydrophobic substituent(s) on the five-membered aromatic ring may further improve binding affinity to the BRD4 protein. Indeed, **14** and **15** with dimethyl substituents on the 3-isoxazole and 3-(1*H*-pyrazole) groups are both more potent than the unsubstituted compounds **9** and **10**. Compound **14** is 9−10 times more potent than **9**, and **15** is 3−7 times more potent than **10** in binding to both the BD1 and BD2 proteins from BRD4. In particular, **15** has K_i values of 19.7 and 20.2 nM to the BD1 and BD2 proteins and is therefore a fairly potent BRD4 inhibitor.

Encouraged by the good binding affinities of **15** to BRD4 BD1 and BD2 proteins, we further modified **15** to obtain **16** and **17**. Compound **16** with an additional methyl substituent on the five-membered 1*H*-pyrazole ring of **15** has similar binding affinities to BRD4 BD1 and BD2 proteins, as compared to **15**, but **17**, which targets the WPF pocket with the same pyrazole group as compound **6**, binds to BRD4 BD1 and BD2 with K_i values of 7.0 nM and 2.7 nM, respectively, and is thus more potent than compound **6**. It is surprising to observe such potency gap between **6** and **17** given these two molecules differ by only one atom, i.e., a carbon to a nitrogen atom.

BET inhibitors such as compounds **1** and **6** have been shown to be very effective in inhibition of cell growth in MV4;11 and MOLM-13 acute leukemia cell lines harboring MLL1 fusions.[3,33] Indeed, **17** potently inhibits cell growth in both the MV4;11 and MOLM-13 cell lines with IC_{50} values of 6 and 36 nM, respectively (Table 3). In direct comparison, **17** is more potent

DOI: 10.1021/acs.jmedchem.7b00193
J. Med. Chem. XXXX, XXX, XXX−XXX

Table 3. Inhibition of Cell Growth by BET Inhibitors in MV4;11 and MOLM-13 Cell Lines

	IC_{50} (nM)			IC_{50} (nM)	
compd	MV4;11	MOLM-13	compd	MV4;11	MOLM-13
1	24 ± 19	56 ± 24	**24**	29	380
4	93 ± 45	241 ± 58	**25**	15	262
5	162 ± 112	228 ± 52	**26**	13 ± 8	139 ± 24
6	20 ± 9	66 ± 14	**27**	>10000	>10000
11	2863	>10000	**28**	>10000	>10000
12	253 ± 123	612 ± 97	**29**	2 ± 1	20 ± 4.6
13	1062	9271	**30**	17 ± 2	69 ± 34
14	182 ± 91	709 ± 116	**31**	26 ± 5	53 ± 11
15	99 ± 36	233 ± 13	**32**	28 ± 13	76 ± 45
16	95 ± 30	193 ± 21	**33**	99 ± 43	220 ± 101
17	6 ± 3	36 ± 2	**34**	47 ± 11	124 ± 78
18	57	205	**35**	295 ± 48	656 ± 240
19	190 ± 89	489 ± 9	**36**	>1000	1140
20	76 ± 31	374 ± 52	**37**	334	NT
21	6.6 ± 1.6	65 ± 11	**38**	77	971
22	5.1 ± 2.8	51 ± 6	**39**	69 ± 13	243 ± 23
23	13 ± 6	127 ± 21	**40**	423	716

than **1**, **5**, and **6** in inhibition of cell growth in these two acute leukemia cell lines and is a very potent BET inhibitor.

We evaluated compound **17** in a quick pharmacokinetic study with three time points to assess its oral exposure in mice. Compound **17** achieves drug concentrations of 2200 ± 331, 872 ± 351, and 72 ± 46 ng/mL, respectively, at 1, 3, and 6 h time points with 25 mg/kg oral administration, indicating that **17** has a reasonable oral exposure in mice.

We next turned our attention to modifications of **12**, which contains a pyrrole ring. Compound **12** has reasonable binding affinities to both BRD4 BD1 and BD2 with K_i values of 51.9 nM and 30.6 nM, respectively, and submicromolar potencies in cell growth inhibition in the MV4;11 and MOML-13 cell lines (Table 3). Our computational modeling suggested that a fused [5,6] bicyclic system can effectively target the WPF pocket, and we therefore synthesized a series of compounds containing a bicyclic [5,6] ring system and whose activities are summarized in Table 4.

Compound **18**, containing an indole group, binds to BRD4 BD1 and BD2 with K_i values of 4.9 nM and 1.1 nM, respectively, and is therefore 10 times more potent than **12** in binding to both the BD1 and BD2 domains of BRD4. Replacement of the indole in **18** with 1*H*-pyrrolo[2,3-*c*]pyridine resulted in **19**, which has a binding affinity to BRD4 BD1 similar to that of **18** but is >5 times less potent than **18** in binding to BDR4 BD2. Installation of a fluorine atom at C4 of the indole in **18** yielded **20**, which binds to BRD4 BD1 and BD2 proteins with very high affinities (K_i < 0.5 nM and 2.6 nM, respectively). Addition of a methyl group at C2 of **18** led to compound **21**, which also achieves a very high binding affinity to both BRD4 BD1 and BD2 (K_i < 1 nM). Combination of the fluorine and methyl substitutions in compounds **20** and **21** yielded **22**, which has a high binding affinity to both BRD4 BD1 and BD2 proteins (K_i < 1 nM). Replacing C6 of the indole group in **21** by a nitrogen atom led to **23**, which is 10 times less potent than **21**. The weaker binding affinity of **23** compared with **21** is consistent with the hydrophobic nature of the WPF binding pocket.

Encouraged by the high binding affinities of these indole-containing compounds, we synthesized a series of compounds containing [5,6] bicyclic, non-indole groups. Compound **24**, with a 2-methylbenzofuran, and compound **25** containing a benzoimidazole bind to BRD4 BD1 and BD2 with high affinities

Table 4. BET Inhibitors Containing [5,6] Fused Aromatic Rings Targeting the WPF Binding Pocket

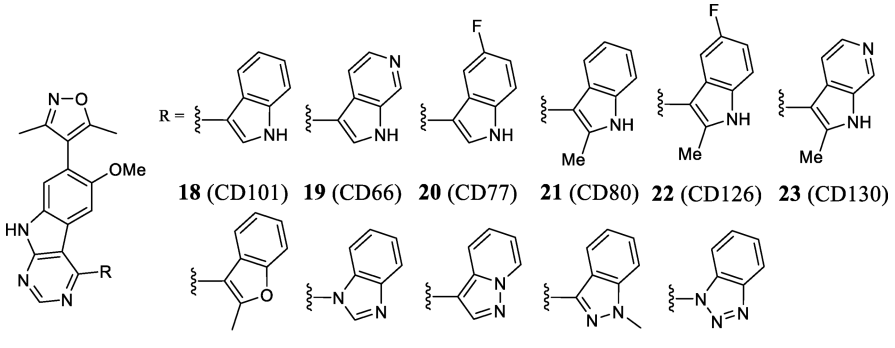

	BRD4 BD2		BRD4 BD1	
compd	IC_{50} (nM)	K_i (nM)	IC_{50} (nM)	K_i (nM)
12	165 ± 50	51.9 ± 18.6	108 ± 37	30.6 ± 9.0
18	20.3 ± 4.9	4.9 ± 2.2	5.5 ± 2.4	1.1 ± 0.7
19	11.6 ± 3.6	7.0 ± 2.4	22.7 ± 7.3	7.1 ± 2.2
20	12.2 ± 4.2	2.6 ± 0.8	2.2 ± 1.0	<0.5
21	5.0 ± 1.7	0.7 ± 0.1	1.1 ± 0.5	<0.5
22	5.6 ± 1.9	0.9 ± 0.3	2.3 ± 1.1	<0.5
23	10.8 ± 3.0	4.2 ± 1.1	25.9 ± 11.8	9.1 ± 4.3
24	32.4 ± 10.2	9.3 ± 3.8	12.2 ± 4.4	2.8 ± 1.1
25	29.4 ± 0.6	9.9 ± 3.3	9.4 ± 2.7	2.8 ± 1.1
26	48.7 ± 17.3	28.0 ± 3.2	26.5 ± 6.1	6.5 ± 0.6
27	147 ± 85	85.1 ± 12.5	74.9 ± 20.7	22.5 ± 6.3
28	>1000	>1000	>1000	>1000

DOI: 10.1021/acs.jmedchem.7b00193
J. Med. Chem. XXXX, XXX, XXX−XXX

Table 5. Pharmacokinetics of Compounds 21 and 31 in Rats and Mice

compd	species	route (dose)	$t_{1/2}$ (h)	C_{max} (ng/mL)	AUC_{0-t} (ng·h/mL)	V_{ss} (L/kg)	CL (L h^{-1} kg^{-1})	F (%)
21	rat	po (25 mg/kg)	1.7	1396.7 ± 277.4	13444.7 ± 933.4		1.9	
31	rat	iv (5 mg/kg)	2.4		6343	2.0	0.79	
	rat	po (25 mg/kg)	2.9	7333	29547		0.88	93
	mouse	iv (5 mg/kg)	0.5		3688.8	2.75	1.36	
	mouse	po (25 mg/kg)	1.60	983.1	9135			50

but are less potent than **18**. Compound **26**, containing a pyrazolo[1,5-*a*]pyridine is 4 times less potent than **18**, and compound **27** containing a 1-methyl-1*H*-indazole is >10 times less potent than **18**. Compound **28** with a 1*H*-benzo[*d*][1,2,3]-triazole fails to show any appreciable binding to BRD4 BD1 and BD2 proteins at 1 μM. These data thus show that not only the shape but also the electronic properties of the bicyclic aromatic rings at this site play an important role in the binding to BRD4 BD1 and BD2 proteins.

We evaluated these compounds for their ability to inhibit cell growth in the MV4;11 and MOML-13 cell lines, and the results are summarized in Table 3. Consistent with their very high binding affinities to BRD4 BD1 and BD2 proteins, compounds **21** and **22** display very potent cell growth inhibitory activity in both the MV4;11 and MOLM-13 cell lines. Compound **21** has IC_{50} values of 6.6 nM and 65 nM, respectively, in the MV4;11 and MOLM-13 cell lines, while **22** has IC_{50} values of 5.1 nM and 51 nM, respectively, in these two leukemia cell lines. Compounds with weaker binding affinities to BRD4 BD1 and BD2 proteins also display weaker cell growth inhibitory activity in both the MV4;11 and MOLM-13 cell lines.

Upon the basis of its high binding affinities to BRD4 BD1 and BD2 proteins and potent cell growth inhibitory activity, we evaluated **21** for its oral bioavailability in rats. The pharmacokinetic (PK) data show that **21** orally administered to rats at 25 mg/kg can achieve a reasonable plasma exposure and achieves a C_{max} of 1396.7 ng/mL, or approximately 3 μM (Table 5).

A shortcoming we discovered in **21** is that although it has a good microsomal stability in rat microsomes ($T_{1/2}$ > 60 min), it has a poor microsomal stability in mouse and human microsomes with $T_{1/2}$ of 4 and 8 min, respectively (Table 6).

Table 6. Microsomal Stability of Selected BET Inhibitors

	microsomal stability $T_{1/2}$ (min)		
compd	mouse	rat	human
21	4	>60	8
29	>60	>60	9
30	>60	>60	>60
31	>60	>60	>60

Our investigation of **21** in human liver microsomes showed that oxidation of the indole group is the major metabolic weak spot, and consequently, we next focused our modifications on the indole group in **21** with the objective of improving its metabolic stability and oral pharmacokinetics.

First, we introduced a methyl group onto the tricyclic core structure in **21**, generating compound **29** (Table 7) which binds to BRD4 BD1 and BD2 proteins with very high affinities (K_i < 1 nM). Consistent with its high binding affinity, **29** potently inhibits cell growth in the MV4;11 and MOML-13 cell lines achieving IC_{50} values of 2 and 20 nM, respectively (Table 3), and is therefore 3 times more potent than **21**. Compound **29** has an excellent microsomal stability in mouse and rat microsomes ($T_{1/2}$ > 60 min) but has a poor microsomal stability in human microsomes ($T_{1/2}$ = 9 min) (Table 6).

We next explored if replacement of the [5,6] bicyclic indole ring system with [6,6] bicyclic ring systems could lead to potent BET inhibitors with improved metabolic stability. Another issue we have found for compound **21** was its poor aqueous solubility. We have synthesized a series of compounds containing a quinoline ring system, which has a basic nitrogen in the bicyclic aromatic system and should have an improved solubility over compound **21** containing a less basic indole aromatic group. The test data from these compounds are summarized in Table 7.

Compound **31** (CD161) containing a quinolin-4-yl ring binds to BRD4 BD1 and BD2 with K_i values of 8.2 nM and 1.4 nM, respectively (Table 7), and potently inhibits cell growth in the MV4;11 and MOLM-13 cell lines with IC_{50} values of 26 and 53 nM, respectively (Table 3). Significantly, **31** has excellent microsomal stability in mouse, rat and human microsomes (Table 6). These data show that replacing the [5,6] bicyclic indole ring system with a [6,6] bicyclic quinoline ring system can maintain high binding affinities to BRD4 BD1 and BD2 and at the same time achieve potent cell growth inhibitory activity and excellent microsomal stability.

Upon the basis of these encouraging results for **31**, we synthesized a series of compounds containing quinoline ring systems in which the nitrogen in the quinoline ring is located in different positions. Compound **34** containing a quinolin-3-yl system is slightly less potent than **31** in binding affinities to BRD4 BD1 and BD2 and also in inhibition of cell growth in the MV4;11 and MOLM-13 cell lines. Similarly, **32** with a quinolin-5-yl system is slightly less potent in its binding to BRD4 BD1 and BD2 proteins than **31** and is 2 times less potent than **31** in inhibition of cell growth in MV4;11 and MOLM-13 cell lines (Table 3). Compounds **35**, **36**, and **37** containing a nitrogen in the 5, 6, and 7 positions, respectively, are much less potent than **31** in both their binding affinities to BRD4 BD1 and BD2 proteins, as well as in inhibition of cell growth. Hence, among these compounds containing a quinolinyl ring system, **31** has the best binding affinities and cellular potencies.

We evaluated **31** for its pharmacokinetics in rats with the data provided in Table 5. At 25 mg/kg, orally administered, compound **31** achieves a C_{max} of 7333 ng/mL, 6 times higher than that for **21**, and an oral bioavailability of 93%. Compound **31** was also found to have much better solubility than **21**; while **31** was readily soluble in the dosing vehicle (5% DMSO + 10% Cremophor + 85% saline), **21** was difficult to dissolve in the vehicle. One possible reason for the superior oral pharmacokinetics of **31** over **21** may be due to the improved solubility for **31**. We further determined the pharmacokinetics of **31** in mice (Table 5). Compound **31** achieves a C_{max} of 983.1 ng/mL with 25 mg/kg oral administration and an oral bioavailability of 50% (Table 5). Hence, **31** has excellent oral pharmacokinetics in rats and moderate oral pharmacokinetics in mice.

To gain an understanding of its target selectivity, we evaluated compound **31** for its binding affinities to BET family proteins

DOI: 10.1021/acs.jmedchem.7b00193
J. Med. Chem. XXXX, XXX, XXX−XXX

Table 7. BET Inhibitors Containing Indole or Quinoline To Target the WPF Pocket

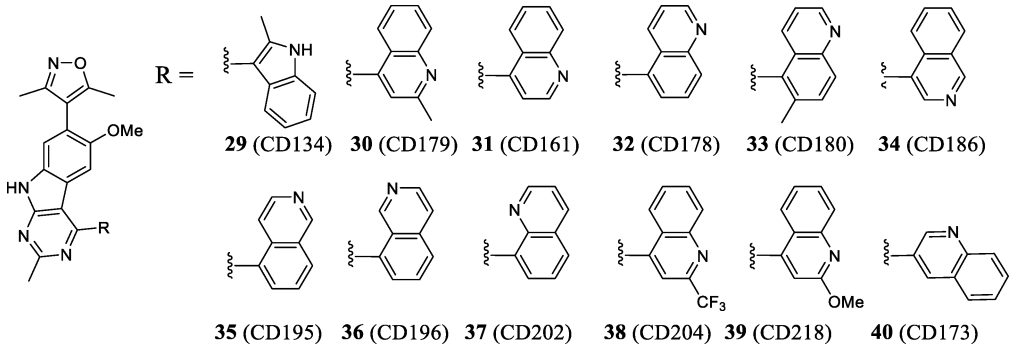

	BRD4 BD2		BRD4 BD1	
compd	IC_{50} (nM)	K_i (nM)	IC_{50} (nM)	K_i (nM)
29	1.9 ± 0.7	<0.5	6.1 ± 1.4	0.8 ± 0.1
30	5.2 ± 1.4	1.6 ± 0.5	19.7 ± 7.5	5.7 ± 3.6
31	7.2 ± 1.9	1.4 ± 0.4	28.2 ± 4.4	8.2 ± 1.2
32	15.5 ± 4.7	3.1 ± 1.0	30.9 ± 7.6	10.1 ± 4.0
33	36.3 ± 6.9	10.5 ± 1.9	93.8 ± 15.8	38.4 ± 10.5
34	12.7 ± 5.9	3.8 ± 0.9	35.6 ± 8.8	9.5 ± 2.4
35	436 ± 219	146 ± 56	451 ± 128	139 ± 32
36	167 ± 55	52.3 ± 17.1	316 ± 86	78.6 ± 12.6
37	193 ± 53	58.2 ± 12.6	412 ± 126	129 ± 24
38	92.7 ± 36.7	26.9 ± 12.6	393 ± 115	122 ± 34
39	14.6 ± 6.3	4.2 ± 1.4	73.1 ± 12.9	31.8 ± 5.9
40	128 ± 27	42.6 ± 6.9	397 ± 47	136 ± 12

Table 8. Binding Affinities of 31 to Different BET Proteins and Selectivity over Other Bromodomain-Containing Proteins, As Determined Using the DiscoverX BROMO Scan Platform

protein	K_d (nM)	protein	K_d (nM)	protein	K_d (nM)
BRD2 (BD1)	4.5	CREBBP	520	BRPF1	>4000
BRD2 (BD2)	0.9	CECR2	1600	BRPF3	>4000
BRD2 (BD1-BD2)	1.1	EP300	550	FALZ	>4000
BRD3 (BD1)	2.0	ATAD2A	>4000	GCN5L2	>4000
BRD3 (BD2)	0.69	ATAD2B	>4000	PBRM1(2)	>4000
BRD3 (BD1-BD2)	0.73	BAZ2A	>4000	PBRM1(5)	>4000
BRD4 (BD1)	8.4	BAZ2B	>4000	PCAF	>4000
BRD4 (BD2)	2.0	BRD1	>4000	SMARCA2	>4000
BRD4 (BD1-BD2)	1.8	BRD7	>4000	SMARCA4	>4000
BRDT (BD1)	15	BRD8 (BD1)	>4000	TAF1 (BD2)	>4000
BRDT (BD2)	5.5	BRD8 (BD2)	>4000	TRIM24	>4000
BRDT (BD1-BD2)	9.7	BRD9	>4000	WDR9 (BD2)	>4000

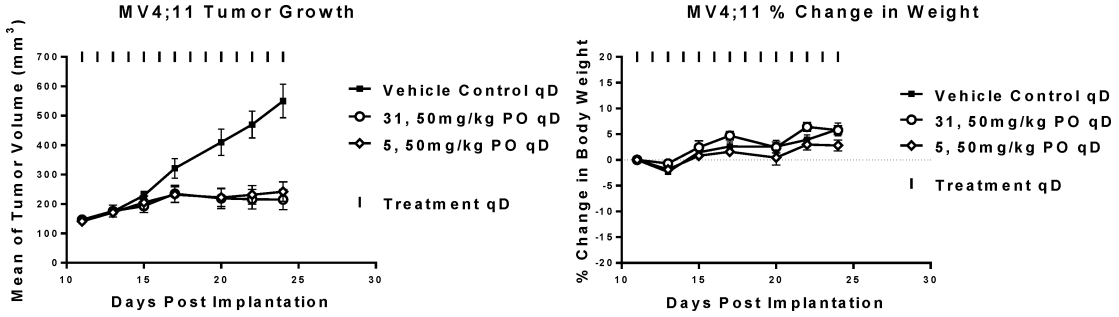

Figure 2. Antitumor activity of **31** in the MV4;11 acute leukemia xenograft model, with compound **5** included as a control.

(BRD2−4 and BRDT) and other subfamilies of bromodomain-containing proteins in the BROMOScan platform by DiscoverX,[34] and the data are summarized in Table 8.

Compound **31** has K_d values of 4.5, 0.9, 2, 0.69, 8.4, 2, 15, and 5.5 nM to BRD2 BD1, BRD2 BD2, BRD3 BD1, BRD3 BD2, BRD4 BD1, BRD4 BD2, BRDT BD1, and BRDT BD2 proteins, respectively. It binds to CREBBP, EP300, and CECR2 with K_d values of 520, 550, and 1600 nM, respectively, and has K_d values of >4000 nM against other 21 bromodomain-containing proteins tested. Hence, **31** is a highly potent BET inhibitor and

DOI: 10.1021/acs.jmedchem.7b00193
J. Med. Chem. XXXX, XXX, XXX−XXX

Table 9. Inhibition of Cell Growth by Compound 31 in a Panel of Breast Cancer Cell Lines

cell line	subtype	IC_{50} (nM)	cell line	subtype	IC_{50} (nM)
MDA-MB-157	basal B	39	HCC1954	basal A	1604
MDA-MB-453	luminal	188	HCC70	basal A	1623
MDA-MB-361	luminal	189	MDA-MB-436	basal B	1698
MDA-MB-231	basal B	244	MDA-MB-468	basal A	1018
HCC38	basal B	285	BT-20	basal A	1713
HCC1428	luminal	319	SUM-159PT	basal B	>2000
BT-474	luminal	434	HBL100	basal B	>2000
BT-549	basal B	410	HCC1143	basal A	>2000
SUM-149PT	basal B	601	HCC1937	basal A	>2000
HCC1395	basal B	1233			

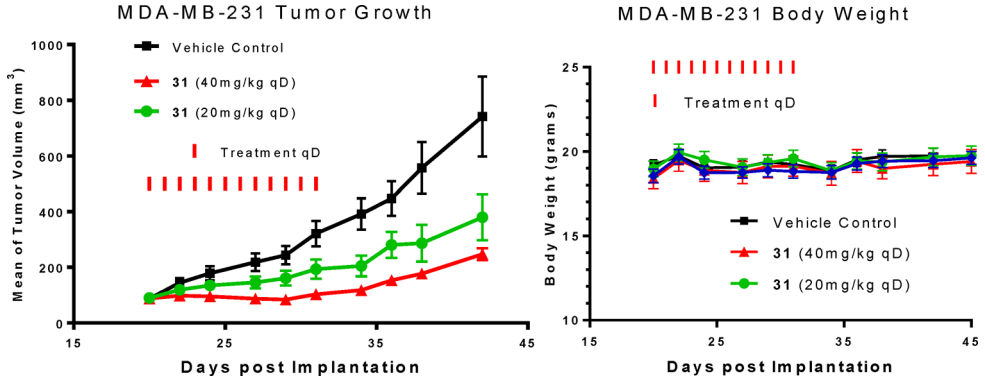

Figure 3. Antitumor activity of **31** in the MDA-MB-231 breast cancer xenograft in mice.

demonstrates a high selectivity over the other bromodomain-containing proteins.

Compound **31** was further tested for its potential inhibitory activity against 372 human kinases in the KINOMEscan platform by DiscoverX. The kinase screening data showed that **31** only has a modest inhibitory activity against PLK4 with an IC_{50} value of 3.9 μM and has IC_{50} values of >50 μM against all other 371 kinases.

We next tested compound **31** for its in vivo efficacy in the MV4;11 xenograft model, with compound **5** used as a control (Figure 2). The efficacy data showed that both **5** and **31** have similar strong antitumor activity with a tumor growth inhibition of >80%, and both compounds did not cause weight loss or other signs of toxicity in mice (Figure 2).

In addition to acute leukemia cell lines, we evaluated the cell growth inhibitory activity of **31** in a panel of 19 human breast cancer cell lines. The resulting data, provided in Table 9, show that **31** potently inhibits cell growth in nine breast cancer cell lines with IC_{50} values of <1 μM, displays IC_{50} values between 1 and 2 μM in six other cell lines, and has IC_{50} values of >2 μM in the remaining four cell lines. Therefore, while **31** is less potent against breast cancer cell lines than against acute leukemia MV4;11 and MOLM-13 cell lines carrying MLL1 fusion, it nevertheless potently inhibits cell growth against nearly 50% of 19 breast cancer cell lines tested with IC_{50} values of 1 μM or better.

To further evaluate its therapeutic potential, we evaluated **31** for its antitumor activity in the MDA-MB-231 xenograft model in mice (Figure 3). The data show that **31** is very effective in inhibition of tumor growth in the MDA-MB-231 xenograft model. During the treatment period, **31** at 40 mg/kg dosing daily achieved essentially complete tumor growth inhibition. Mice treated with **31** did not experience weight loss or other signs of toxicity throughout the entire experiment.

Previous studies have shown that BET inhibitors can effectively down-regulate c-Myc and up-regulate p21 in tumor cells.[4] Accordingly, we examined the effect of **31** in the MV4;11 cells on c-Myc and p21 levels (Figure 4). The resulting data

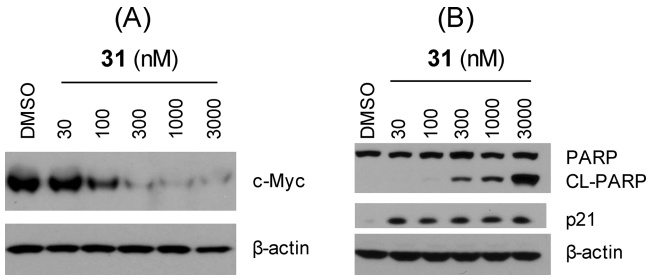

Figure 4. Western blot analysis of the effect of compound **31** on c-Myc, PARP and p21 in the MV4;11 leukemia cells. (A) MV4;11 cells were treated with different concentrations of **31** for 1 h, and c-Myc protein was probed by a specific antibody. (B) MV4;11 cells were treated with compound **31** for 24 h, and PARP, cleaved PARP (CL-PAPR), and p21 proteins were probed by specific antibodies. β-Actin was used as the loading control.

showed that **31** is very effective in inducing rapid down-regulation of c-Myc at as early as the 1 h time point and in a dose-dependent manner (Figure 4A). Furthermore, compound **31** is effective in inducing up-regulation of the cell cycle regulator p21 and cleavage of PARP, a biochemical marker of apoptosis, in a dose-dependent manner (Figure 4B). Hence, our Western blotting data further showed that compound **31** functions as a potent BET inhibitor in cells.

To understand the structural basis for the high binding affinity of **31** to BRD4, we successfully determined the cocrystal structure of **31** complexed with BRD4 BD2 (Figure 5). Overall, the

DOI: 10.1021/acs.jmedchem.7b00193
J. Med. Chem. XXXX, XXX, XXX−XXX

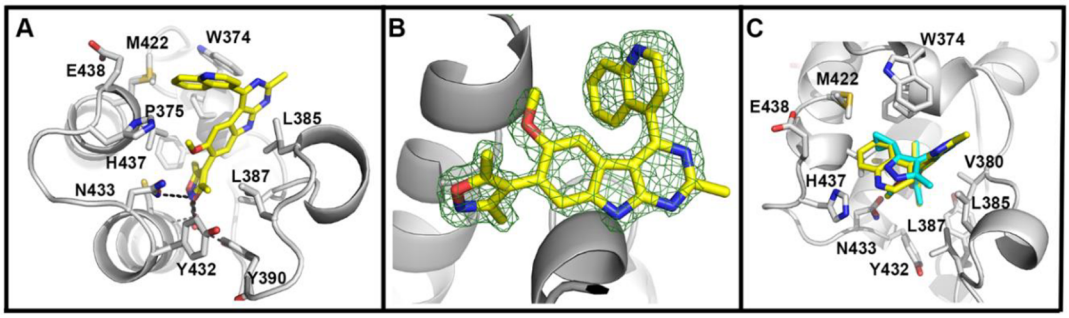

Figure 5. Crystal structure of BRD4 BD2 bound to **31** determined at 2.5 Å resolution. (A) BRD4 BD2 is shown as a gray cartoon with its side chains interacting with **31** shown as sticks (carbon atoms in gray, nitrogens in blue, oxygens in red, and sulfurs in gold). **31** is shown as sticks in the same coloring as the protein except carbon atoms are in yellow. (B) The omit $F_o - F_c$ electron density map for compound **31** shown as a green grid contoured at 3σ. (C) Previously determined crystal structure of BRD4 BD2 complexed with **6** overlaid onto the cocrystal structure of BRD4 BD2 complexed with **31**. Panel C is rotated 90° about the *x*-axis with respect to panel A. Compound **6** is shown as sticks with carbon atoms in cyan.

cocrystal structure shows **31** binding to BRD4 BD2 with a binding mode similar to that assumed by compound **6**. The dimethylisoxazole group of **31** penetrates deeply into the binding pocket and forms an extensive hydrogen bonding network with Asn433 and two conserved water molecules. One of the methyl groups in the dimethylisoxazole group binds to a hydrophobic pocket formed by residues Tyr332, Val380, Leu387, and Tyr390, and the other methyl group has hydrophobic contacts with Pro375, Phe376, and Val439. The tricyclic ring binds to the lysine channel. As envisaged in our design, the quinolinyl group inserts into the "WPF" pocket with the nitrogen atom exposed to solvent and the fused phenyl group in the hydrophobic pocket formed by Trp374, Pro375, Val439, Met442 and the hydrophobic portion of Glu438. The quinolinyl group of **31** has more extensive interactions than the cyclopropyl group of **6**, consistent with the higher binding potency of **31** to BRD4.This cocrystal structure provides a solid structural basis for the high binding affinity of **31** to BRD4 BD2 and for further structure-based optimization.

CHEMISTRY

The synthesis of 9*H*-pyrimido[4,5-*b*]indole-containing intermediate **7** is shown in Scheme 1.

Suzuki coupling of a previously reported substituted bromobenzene (**S1**) and its regioisomer 1-bromo-2-fluoro-4-methoxy-5-nitrobenzene (ratio 2:1)[35] and **S2** furnished **S3** as a mixture of two isomers in >80% yield. SN_{Ar} substitution of the fluorine of **S3** by the cynoacetate carbanion afforded **S5**, which was obtained as a single isomer after flash column chromatography purification. **S5** was reduced, giving **S6** by treatment with Zn-HOAc at 85 °C.[36] Condensation of a mixture of **S6** and ammonium formate in formamide at 175 °C yielded **S7** in 55% yield. Finally, chlorination of **S7** provided the final key intermediate (**7**) in 66% yield.

The key 9*H*-pyrimido[4,5-*b*]indole-containing intermediate **S10** was synthesized from **S6** following the synthetic route depicted in Scheme 2.[36]

To a dry solution of **S6** in MeCN, excess hydrogen chloride gas was bubbled, and the mixture was heated at reflux for 2.5 h. Removal of the volatile components furnished the crude intermediate **S8**, which cyclized into **S9** upon reflux in basic aqueous EtOH. Chlorination of **S9** provided the key intermediate **S10** in 75% yield.

Compound **8** in Table 1 was synthesized following the synthetic route depicted in Scheme 3.

Scheme 3. Synthesis of 8[a]

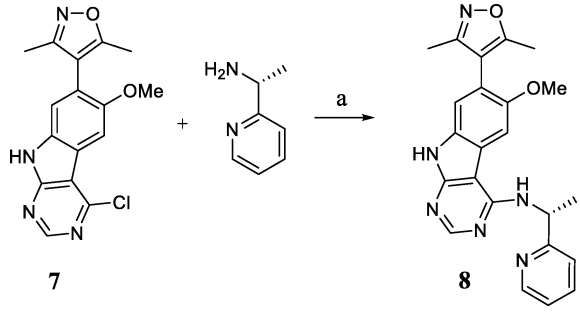

[a]Reaction conditions: (a) 1-methylpyrrolidin-2-one (NMP), 140 °C, overnight.

An anhydrous solution in NMP of **7** and the corresponding amine was heated at 140 °C in a sealed tube overnight. The final products (**8**) were purified by reverse phase HPLC and obtained in the form of the trifluoroacetic acid salt. Compounds **13** and **25** were synthesized in a similar manner.

Compounds **9**–**12**, **14**–**24**, **26**, **27**, **29**–**40** in Tables 2–4 and 7 were synthesized from key intermediates **7** or **S10** as shown in Scheme 4.

Scheme 4. General Suzuki Coupling Reaction Conditions[a]

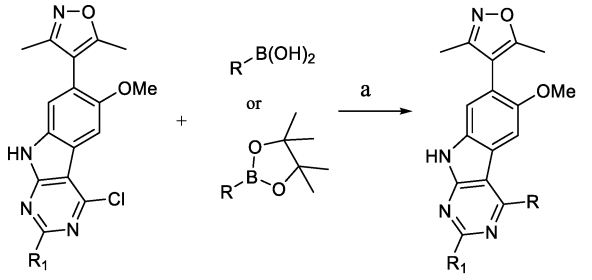

[a]Reaction conditions: (a) $Pd(PPh_3)_4$, DME–H_2O, K_2CO_3 5.0 equiv, reflux overnight; or $Pd(dppf)_2Cl_2$–CH_2Cl_2, DME–Na_2CO_3 2 M, reflux overnight.

Most boronic acids or pinacolboronic esters are commercially available. Others were synthesized according to known methods reported previously.[37−39] Suzuki coupling[37,40,41] of the corresponding boronic acids or pinacolboronic esters and **7** or **S10**

DOI: 10.1021/acs.jmedchem.7b00193
J. Med. Chem. XXXX, XXX, XXX−XXX

followed by reverse phase HPLC purification furnished pure final products as salts of trifluoroacetic acid.

Compound **28** was synthesized from **7** and 1*H*-benzo[*d*][1,2,3]triazole following a literature reported method with modifications.[42]

CONCLUSIONS

In this study, we have designed and synthesized a class of 9*H*-pyrimido[4,5-*b*]indole-containing compounds with the goal of obtaining potent and orally bioavailable BET bromodomain inhibitors. These efforts have led to the discovery of 4-(6-methoxy-2-methyl-4-(quinolin-4-yl)-9*H*-pyrimido[4,5-*b*]indol-7-yl)-3,5-dimethylisoxazole (**31**), which binds to BET family proteins with low nanomolar affinities and demonstrates high selectivity over non-BET bromodomain-containing proteins. Compound **31** potently inhibits cell growth in acute leukemia cell lines and breast cancer cell lines. Significantly, it achieves excellent oral bioavailability and is metabolically stable. It also displays potent antitumor activity in MV4;11 acute leukemia and MDA-MB-231 breast cancer xenograft models in mice at well-tolerated dose-schedules. Compound **31** is a potent, selective, orally bioavailable, and efficacious BET inhibitor.

EXPERIMENTAL SECTION

Chemistry. General Methods. All reactions were conducted in a round-bottom flask equipped with a Teflon-coated magnet stirring bar. Experiments involving components sensitive to moisture or air were performed under a nitrogen atmosphere. Commercially available reagents and anhydrous solvents were used without further purification. The crude reaction product was purified by flash column chromatography packed with silica gel. Further purification was performed on a preparative HPLC (Waters 2545) with a C18 reverse phase column. The mobile phase was a gradient flow of solvent A (water, 0.1% of TFA) and solvent B (CH_3CN, 0.1% of TFA) at a flow rate of 30 mL/min. Proton nuclear magnetic resonance (^{1}H NMR) and carbon nuclear magnetic resonance (^{13}C NMR) spectroscopies were performed in Bruker Advance 300 NMR spectrometers. Low resolution ESI mass spectrum analysis was performed on a Thermo-Scientific LCQ Fleet mass spectrometer. The analytical UPLC model was Waters ACQUITY H class (UV detection at 230 and 254 nm wavelengths), and the reverse phase column used was the ACQUITY UPLC BEH (C18, 1.7 μm, 2.1 mm × 50 mm). All final compounds were purified to ≥95% purity as determined by analytical UPLC analysis.

1. Procedures for the Synthesis of 9*H*-pyrimido[4,5-*b*]indole-Containing Cores 7 and S10. 4-(4-Fluoro-2-methoxy-5-nitrophenyl)-3,5-dimethylisoxazole (S3). 1-Bromo-4-fluoro-2-methoxy-5-nitrobenzene[35] and 1-bromo-2-fluoro-4-methoxy-5-nitrobenzene (3 g, 12 mmol, 2:1 ratio), 3,5-dimethyl-4-(4,4,5,5-tetramethyl-1,3,2-dioxaborolan-2-yl)isoxazole (5.35 g, 24 mmol), and K_2CO_3 (5.0 g, 36 mmol) were added to a round-bottom flask. DME (50 mL) and water (30 mL) were added at room temperature. The solution was degassed before addition of $Pd(PPh_3)_4$ (700 mg, 0.6 mmol) in one portion. The solution was degassed and was then heated at reflux for 16 h. The aqueous layer was extracted with EtOAc, and combined organic layers were washed with brine and dried over anhydrous Na_2SO_4. The volatile components were removed on a rotary evaporator, and the residue was purified by flash column chromatogram. The desired product (**S3**) and its regioisomer were isolated in >80% yield (3.38 g). **S3**: ^{1}H NMR ($CDCl_3$, 300 MHz) 8.03 (d, J = 8.47 Hz, 1H), 6.93 (d, J = 12.56 Hz, 1H), 4.00 (s, 3H), 2.40 (s, 3H), 2.24 (s, 3H).

Ethyl 2-Cyano-2-(4-(3,5-dimethylisoxazol-4-yl)-5-methoxy-2-nitrophenyl)acetate (S5). NaH (4.32 g, 60% in mineral oil, 100 mmol, 2.0 equiv) was placed in round-bottom flask, and dry DMF (200 mL) was added. Ethyl cyanoacetate (7.35 g, 65 mmol, 1.2 equiv) was added dropwise at 0 °C via a syringe. The solution was stirred at room temperature for 30 min. The mixture was cooled to 0 °C, and anhydrous DMF solution (30 mL) of **S3** and its regioisomer (14.26 g, 54 mmol, 1.0 equiv) was added via a syringe. The reaction mixture was allowed to warm up to room temperature and was then stirred for 16 h. The reaction was quenched by 0.5 N HCl, and the aqueous layer was extracted with EtOAc, the combined organic layers were washed with brine, then dried over anhydrous Na_2SO_4. The volatile components were removed on a rotary evaporator, and the residue was purified by flash column chromatogram. Pure **S5** was isolated in 53% yield (6.86 g, 19.1 mmol, based on 66% correct isomer). ^{1}H NMR ($CDCl_3$, 300 MHz): 8.10 (s, 1H), 7.27 (s, 1H), 5.78 (s, 1H), 4.35 (q, J = 7.12 Hz, 2H), 3.99 (s, 3H), 2.33 (s, 3H), 2.18 (s, 3H), 1.37 (t, J = 7.14 Hz, 3H). ^{13}C NMR ($CDCl_3$, 75 MHz): 167.2, 163.6, 161.6, 159.2, 140.0, 129.7, 128.0, 121.6, 114.7, 112.8, 110.7, 64.0, 56.7, 42.0, 14.0, 11.7, 10.8. ESI-MS calculated for $C_{17}H_{18}N_3O_6$ $[M + H]^+$ = 360.12. Observed: 360.58

Ethyl 2-Amino-6-(3,5-dimethylisoxazol-4-yl)-5-methoxy-1*H*-indole-3-carboxylate (S6). To a solution of **S5** (6.86 g, 19.1 mmol, 1.0 equiv) in AcOH (50 mL) at 85 °C, Zn powder (2.6 g, 40 mmol, 2.0 equiv) was added in small portions. The mixture was stirred at 85 °C for 1 h, a further 2.6 g of Zn powder (40 mmol, 2.0 equiv) was added, and the reaction was kept at the same temperature for 2 h. The reaction was cooled, filtered, and washed with AcOH. The AcOH solution was combined, and the volatile components were removed on a rotary evaporator. Purification by flash column chromatogram furnished the desired product **S6** (2.62 g, ∼47% yield based on recovering 13% starting material). ^{1}H NMR ($CDCl_3$, 300 MHz): 8.01 (br, s, 1H), 7.44 (s, 1H), 6.78 (s, 1H), 5.73 (br, s, 2H), 4.40 (q, J = 7.08 Hz, 2H), 3.82 (s, 3H), 2.29 (s, 3H), 2.15 (s, 3H), 1.45 (t, J = 7.08 Hz, 3H). ^{13}C NMR ($CDCl_3$, 75 MHz): 167.2, 165.8, 160.6, 153.7, 153.1, 128.1, 126.7, 114.5, 112.0, 110.6, 101.8, 86.0, 55.6, 53.5, 14.7, 11.5, 10.6. ESI-MS calculated for $C_{17}H_{20}N_3O_4$ $[M + H]^+$ = 330.15. Obtained: 330.25

7-(3,5-Dimethylisoxazol-4-yl)-6-methoxy-9*H*-pyrimido[4,5-*b*]indol-4-ol (S7). S6 (0.45 g, 1.4 mmol), ammonium formate (1.06 g, 17 mmol), and formamide (16 mL) were heated at 175 °C for 16 h. The reaction mixture was cooled to room temperature, and water was added. Filtration of the mixture yielded **S7** as a brown solid (0.24 g, 0.77 mmol, 55% yield). ^{1}H NMR (DMSO-d_6, 300 MHz): 8.09 (s, 1H), 7.57 (s, 1H), 7.24 (s, 1H), 3.81 (s, 3H), 3.30 (s, 1H), 2.62 (s, 3H), 2.06 (s, 3H). ^{13}C NMR (DMSO, 75 MHz): 165.3, 162.9, 159.2, 158.3, 153.9, 152.5, 129.6, 122.7, 115.6, 114.1, 113.6, 102.0, 100.2, 55.5, 11.2, 10.3. ESI-MS calculated for $C_{16}H_{15}N_4O_3$ $[M + H]^+$: 311.11. Obtained: 311.75.

4-(4-Chloro-6-methoxy-9*H*-pyrimido[4,5-*b*]indol-7-yl)-3,5-dimethylisoxazole (7, CD55). S7 (0.95 g, 3.05 mmol) was dissolved in $POCl_3$ (15 mL), and the mixture was heated at 90 °C for 5 h. The mixture was cooled to room temperature, and the volatile components were removed on a rotary evaporator. The $POCl_3$ solution was poured into EtOAc (40 mL), followed by saturated $NaHCO_3$ (60 mL) and water (100 mL). The mixture was quickly filtered, and the desired product (**7**) was collected as a brown solid (0.3 g). The aqueous layer was extracted with EtOAc and the combined organic layers were washed with brine and dried over anhydrous Na_2SO_4. The volatile components were removed on a rotary evaporator affording a brown solid (0.36 g). The total yield of **7** is 66% (0.66 g). ^{1}H NMR (DMSO-d_6, 300 MHz): 8.74 (s, 1H), 7.84 (s, 1H), 7.45 (s, 1H). 3.89 (s, 3H), 3.31 (br, s, 1H), 2.29 (s, 3H), 2.09 (s, 3H). ^{13}C NMR (DMSO-d_6, 75 MHz): 167.8, 161.2, 155.8, 122.2, 120.3, 117.0, 115.2, 113.1, 105.8, 57.8, 13.4, 12.4. ESI-MS calculated for $C_{16}H_{14}{}^{35}ClN_4O_2$ $[M + H]^+$ = 329.08. Obtained: 329.67.

7-(3,5-Dimethylisoxazol-4-yl)-6-methoxy-2-methyl-9*H*-pyrimido[4,5-*b*]indol-4-ol (S9). To a round-bottom flask, **S6** (0.37 g, 1.1 mmol) and MeCN (20 mL) were added at room temperature. Dry HCl was bubbled through MeCN for 30 min, and the reaction mixture was heated at reflux for 2.5 h. The reaction was then cooled to room temperature, and the volatile components were removed on a rotary evaporator. To this crude mixture, 10% NaOH aqueous solution (20 mL) and EtOH (50 mL) were added, and the solution was heated at reflux for 6 h. The volatile components were then removed on a rotary evaporator, and the aqueous residue was acidified with 2 N HCl aqueous solution. The product **S9** was allowed to precipitate at 0 °C. Filtration of the mixture furnished **S9** in 0.278 g (78% yield, 2 steps). ^{1}H NMR (DMSO-d_6, 300 MHz): 7.57 (s, 1H), 7.20 (s, 1H), 3.81 (s, 3H), 2.37

DOI: 10.1021/acs.jmedchem.7b00193
J. Med. Chem. XXXX, XXX, XXX−XXX

(s, 3H), 2.27 (s, 3H), 2.08 (s, 3H). ^{13}C NMR (DMSO-d_6, 75 MHz): 165.2, 160.4, 159.4, 157.7, 155.4, 152.2, 130.0, 123.2, 114.5, 114.0, 113.8, 101.9, 97.9, 55.6, 21.9, 11.3, 10.4.

4-(4-Chloro-6-methoxy-2-methyl-9*H*-pyrimido[4,5-*b*]indol-7-yl)-3,5-dimethylisoxazole (S10). **S9** (0.278 g, 0.8 mmol) and $POCl_3$ (8 mL) were added to a round-bottom flask. The mixture was heated at 90 °C for 6 h. The reaction mixture was cooled to room temperature, and the volatile components were removed on a rotary evaporator. Water (20 mL) and EtOAc (20 mL) were added, and the pH was adjusted to 8 using a large excess of $NaHCO_3$ saturated aqueous solution. Rapid filtration of the mixture furnished **S10** as a brown solid in 0.208 g (75% yield). ^{1}H NMR (DMSO-d_6, 300 MHz): 7.81 (s, 1H), 7.43 (s, 1H), 3.89 (s, 3H), 2.69 (s, 3H), 2.31 (s, 3H), 2.11 (s, 3H). ^{13}C NMR (DMSO-d_6, 75 MHz): 165.8, 163.6, 159.2, 156.9, 152.5, 151.1, 132.5, 119.5, 118.3, 114.7, 113.2, 108.5, 103.6, 55.8, 25.5, 11.3, 10.4. ESI-MS calculated for $C_{17}H_{16}{}^{35}ClN_4O_2$ $[M + H]^+$ = 343.10. Obtained: 343.58.

2. Synthesis of Final Products. 7-(3,5-Dimethylisoxazol-4-yl)-6-methoxy-*N*-((*R*)-1-(pyridin-2-yl)ethyl)-9*H*-pyrimido[4,5-*b*]indol-4-amine (8). **7** (80 mg, 0.3 mmol), (*R*)-1-(pyridin-2-yl)-ethanamine (122 mg, 1 mmol), and EtN(*i*-Pr)$_2$ (0.3 mL, 1.5 mmol) were added to a round-bottomed flask. NMP (3 mL) was added at room temperature. The solution was heated at 140 °C for 16 h. The reaction mixture was quenched by water (1 mL). The mixture was purified by reverse phase HPLC. The desired product **8** was isolated as a salt of CF_3CO_2H (16 mg, 20%). ^{1}H NMR (MeOD-d_4, 300 MHz): 8.81 (d, J = 5.58 Hz, 1H), 8.54 (s, 1H), 8.56−8.47 (m, 1H), 8.23−8.17 (m, 1H), 8.19 (s, 1H), 7.92 (t, J = 6.39 Hz, 1H), 7.50 (s, 1H), 6.00 (q, J = 7.11 Hz, 1H), 4.02 (s, 3H), 2.33 (s, 3H), 2.16 (s, 3H), 2.00 (d, J = 7.11 Hz, 3H). ESI-MS calculated for $C_{23}H_{23}N_6O_2$ $[M + H]^+$ = 415.19. Obtained: 415.92.

4-(4-(Isoxazol-4-yl)-6-methoxy-9*H*-pyrimido[4,5-*b*]indol-7-yl)-3,5-dimethylisoxazole (9). Method I using **7** and 4-(4,4,5,5-tetramethyl-1,3,2-dioxaborolan-2-yl)isoxazole: 13% yield. ^{1}H NMR (300 MHz, MeOD-d_4): 9.73 (s, 1H), 9.22 (s, 1H), 9.07 (s, 1H), 7.57 (s, 1H), 7.55 (s, 1H), 3.87 (s, 3H), 2.33 (s, 3H), 2.16 (s, 3H). ESI-MS calculated for $C_{19}H_{16}N_5O_3$ $[M + H]^+$ = 362.13. Obtained: 362.58.

4-(6-Methoxy-4-(1*H*-pyrazol-4-yl)-9*H*-pyrimido[4,5-*b*]indol-7-yl)-3,5-dimethylisoxazole (10),. Method I using **7** and 4-(4,4,5,5-tetramethyl-1,3,2-dioxaborolan-2-yl)-1*H*-pyrazole: 41% yield. ^{1}H NMR (300 MHz, MeOD-d_4): 9.09 (s, 1H), 8.61 (s, 2H), 7.79 (s, 1H), 7.60 (s, 1H), 3.87 (s, 3H), 2.33 (s, 3H), 2.15 (s, 3H). ESI-MS calculated for $C_{19}H_{17}N_6O_2$ $[M + H]^+$ = 361.14. Obtained: 361.50.

Method A: Synthesis of 4-(4-(Furan-3-yl)-6-methoxy-9*H*-pyrimido[4,5-*b*]indol-7-yl)-3,5-dimethylisoxazole (11). For Suzuki coupling catalyzed by $Pd(PPh_3)_4$: **7** (33 mg, 0.1 mmol, 1.0 equiv), 2-(furan-3-yl)-4,4,5,5-tetramethyl-1,3,2-dioxaborolane (60 mg, 0.3 mmol, 3.0 equiv), and K_2CO_3 (56 mg, 0.4 mmol, 4.0 equiv) were added to a round-bottom flask. DME (6 mL) and H_2O (4 mL) were added at room temperature. The solution was degassed before $Pd(PPh_3)_4$ (10−15 mg, 0.008−0.012 mmol, ∼0.1 equiv) was added in one portion. The solution was degassed again and then was heated at reflux for 16 h. The aqueous layer was extracted with EtOAc, and combined organic layers were washed with brine and dried over anhydrous Na_2SO_4. The volatile components were removed on a rotary evaporator and the residue was treated with TFA (0.5 mL) and then purified by reverse phase HPLC. **11** was isolated as a colorless solid in the form of TFA salt (14 mg, 39% yield). ^{1}H NMR (MeOD-d_4, 300 MHz): 9.10 (s, 1H), 8.61 (dd, J = 1.52, 0.88 Hz, 1H), 8.04 (t, J = 1.52 Hz, 1H), 7.78 (s, 1H), 7.59 (s, 1H), 7.28 (dd, J = 1.91, 0.88 Hz, 1H), 3.86 (s, 3H), 2.33 (s, 3H), 2.16 (s, 3H). ESI-MS calculated for $C_{20}H_{17}N_4O_3$ $[M + H]^+$ = 361.13. Obtained: 361.33.

4-(6-Methoxy-4-(1*H*-pyrrol-3-yl)-9*H*-pyrimido[4,5-*b*]indol-7-yl)-3,5-dimethylisoxazole (12). Method A using *N*-TIPS pyrrole-3-boronic acid pinacol ester: 21% yield. ^{1}H NMR (MeOD-d_4, 300 MHz): 8.95 (s, 1H), 8.08 (s, 1H), 7.93 (t, J = 1.65 Hz, 1H), 7.57 (s, 1H), 7.23 (dd, J = 2.91, 1.81 Hz, 1H), 7.03 (dd, J = 2.91, 1.62 Hz, 1H), 3.87 (s, 3H), 2.34 (s, 3H), 2.17 (s, 3H). ^{13}C NMR (MeOD-d_4, 75 MHz): 168.2, 161.2, 157.6, 155.7, 150.4, 148.4, 135.4, 124.6, 123.5, 123.0, 122.0, 117.0, 115.1, 114.7, 110.6, 110.1, 105.4, 56.5, 11.7, 10.8. ESI-MS calculated for $C_{20}H_{18}N_5O_2$ $[M + H]^+$ = 360.15. Obtained: 360.25.

4-(4-(1*H*-Imidazol-1-yl)-6-methoxy-9*H*-pyrimido[4,5-*b*]indol-7-yl)-3,5-dimethylisoxazole (13). **7** (26 mg, 0.08 mmol), imidazole (60 mg, 0.88 mmol), and anhydrous NMP (10 mL) were heated at 170 °C in sealed tube for 24 h. HPLC purification of the reaction mixture provided the title compound in 27% yield (10 mg). ^{1}H NMR (MeOD-d_4, 300 MHz): 9.73 (s, 1H), 8.95 (s, 1H), 8.46 (s, 1H), 7.93 (s, 1H), 7.53 (s, 1H), 7.47 (s, 1H), 3.85 (s, 3H), 2.33 (s, 3H), 2.15 (s, 3H). ESI-MS calculated for $C_{19}H_{17}N_6O_2$ $[M + H]^+$ =361.14. Obtained: 361.33

4,4′-(6-Methoxy-9*H*-pyrimido[4,5-*b*]indole-4,7-diyl)bis(3,5-dimethylisoxazole) (14). Method A using 3,5-dimethyl-4-(4,4,5,5-tetramethyl-1,3,2-dioxaborolan-2-yl)isoxazole ester: 41% yield. ^{1}H NMR (MeOD-d_4, 300 MHz): 9.15 (s, 1H), 7.58 (s, 1H), 7.08 (s, 1H), 3.79 (s, 3H), 2.51 (s, 3H), 2.32 (s, 3H), 2.31 (s, 3H), 2.15 (s, 3H). ESI-MS calculated for $C_{21}H_{20}N_5O_3$ $[M + H]^+$ = 390.16. Obtained: 390.42.

4-(4-(3,5-Dimethyl-1*H*-pyrazol-4-yl)-6-methoxy-9*H*-pyrimido[4,5-*b*]indol-7-yl)-3,5-dimethylisoxazole (15). Method A using 3,5-dimethylpyrazole-4-boronic acid pinacol ester: 67% yield. ^{1}H NMR (MeOD-d_4, 300 MHz): 9.17 (s, 1H), 7.62 (s, 1H), 7.12 (s, 1H), 3.77 (s, 3H), 2.34 (s, 6H), 2.32 (s, 3H), 2.15 (s, 3H). ^{13}C NMR (MeOD-d_4, 75 MHz): 168.3, 161.1, 157.7, 155.8, 150.3, 148.3, 146.2, 135.7, 123.8, 121.4, 117.2, 114.6, 110.9, 104.9, 56.4, 11.7, 11.6, 10.8. ESI-MS calculated for $C_{21}H_{21}N_6O_2$ $[M + H]^+$ = 389.17. Obtained: 389.83.

4-(6-Methoxy-4-(1,3,5-trimethyl-1*H*-pyrazol-4-yl)-9*H*-pyrimido[4,5-*b*]indol-7-yl)-3,5-dimethylisoxazole (16). Method A using 1,3,5-trimethyl-1*H*-pyrazole-4-boronic acid pinacol ester: 42% yield. ^{1}H NMR (MeOD-d_4, 300 MHz): 9.20 (s, 1H), 7.65 (s, 1H), 7.16 (s, 1H), 3.97 (s, 3H), 3.81 (s, 3H), 2.40 (s, 3H), 2.35 (s, 3H), 2.29 (s, 3H), 2.17 (s, 3H). ESI-MS calculated for $C_{22}H_{23}N_6O_2$ $[M + H]^+$ = 403.19. Obtained: 403.50

4-(4-(3-Cyclopropyl-5-methyl-1*H*-pyrazol-4-yl)-6-methoxy-9*H*-pyrimido[4,5-*b*]indol-7-yl)-3,5-dimethylisoxazole (17). Method A using *tert*-butyl 3-cyclopropyl-5-methyl-4-(4,4,5,5-tetramethyl-1,3,2-dioxaborolan-2-yl)-1*H*-pyrazole-1-carboxylate: 65% yield. ^{1}H NMR (MeOD-d_4, 300 MHz): 9.13 (s, 1H), 7.58 (s, 1H), 7.30 (s, 1H), 3.83 (s, 3H), 2.38 (s, 3H), 2.37 (s, 3H), 2.19 (s, 3H), 1.90−1.70 (m, 1H), 1.10−1.00 (m, 1H), 1.00−0.80 (m, 3H).

4-(4-(1*H*-Indol-3-yl)-6-methoxy-9*H*-pyrimido[4,5-*b*]indol-7-yl)-3,5-dimethylisoxazole (18). Method A using (1-(*tert*-butoxycarbonyl)-1*H*-indol-3-yl)boronic acid: 40% yield. ^{1}H NMR (MeOD-d_4, 300 MHz): 9.06 (s, 1H), 8.27 (s, 1H), 7.71 (d, J = 8.20 Hz, 1H), 7.57 (s, 1H), 7.50 (d, J = 7.96 Hz, 1H), 7.41 (ddd, J = 8.24, 7.21, 1.13 Hz, 1H), 7.29 (ddd, J = 8.03, 7.08, 0.97 Hz, 1H), 7.15 (s, 1H), 3.42 (s, 1H), 2.32 (s, 1H), 2.13 (s, 1H). ESI-MS calculated for $C_{24}H_{20}N_5O_2$ $[M + H]^+$ = 410.16. Obtained: 410.33.

4-(6-Methoxy-4-(1*H*-pyrrolo[2,3-*c*]pyridin-3-yl)-9*H*-pyrimido[4,5-*b*]indol-7-yl)-3,5-dimethylisoxazole (19). Method A using 3-(4,4,5,5-tetramethyl-1,3,2-dioxaborolan-2-yl)-1*H*-pyrrolo-[2,3-*c*]pyridine: 37% yield. ^{1}H NMR (MeOD-d_4, 300 MHz): 9.40 (s, 1H), 9.16 (s, 1H), 9.09 (s, 1H), 8.46 (d, J = 6.54 Hz, 1H), 8.25 (d, J = 6.54 Hz, 1H), 7.58 (s, 1H), 7.19 (s, 1H), 3.58 (s, 3H), 2.32 (s, 3H), 2.14 (s, 3H). ^{13}C NMR (MeOD-d_4, 300 MHz): 168.0, 161.2, 158.1, 154.5, 141.4, 137.1, 135.1, 134.0, 130.9, 130.2, 122.3, 120.9, 119.4, 116.3, 114.9, 113.2, 105.6, 56.3, 11.7, 10.8. ESI-MS calculated for $C_{23}H_{19}N_6O_2$ $[M + H]^+$ = 411.16. Obtained: 411.42.

4-(4-(6-Fluoro-1*H*-indol-3-yl)-6-methoxy-9*H*-pyrimido[4,5-*b*]indol-7-yl)-3,5-dimethylisoxazole (20). Method A using *tert*-butyl 6-fluoro-3-(4,4,5,5-tetramethyl-1,3,2-dioxaborolan-2-yl)-1*H*-indole-1-carboxylate: 44% yield. ^{1}H NMR (MeOD-d_4, 300 MHz): 9.10 (s, 1H), 8.38 (s, 1H), 7.80−7.70 (m, 1H), 7.62 (s, 1H), 7.30−7.10 (m, 3H), 3.52 (s, 3H), 2.35 (s, 3H), 2.16 (s, 3H). ESI-MS calculated for $C_{24}H_{19}FN_5O_2$ $[M + H]^+$ = 428.15. Obtained: 428.25.

4-(6-Methoxy-4-(2-methyl-1*H*-indol-3-yl)-9*H*-pyrimido[4,5-*b*]indol-7-yl)-3,5-dimethylisoxazole (21). Method A using *tert*-butyl 2-methyl-3-(4,4,5,5-tetramethyl-1,3,2-dioxaborolan-2-yl)-1*H*-indole-1-carboxylate: 26% yield. ^{1}H NMR (MeOD-d_4, 300 MHz): 9.12 (s, 1H), 7.61−7.58 (m, 1H), 7.58 (s, 1H), 7.37−7.15 (m, 3H), 6.82 (s, 1H), 3.32 (s, 3H), 2.67 (s, 3H), 2.31 (s, 3H), 2.12 (s, 3H). ESI-MS calculated for $C_{25}H_{22}N_5O_2$ $[M + H]^+$ = 424.18. Obtained: 424.42.

4-(4-(6-Fluoro-2-methyl-1*H*-indol-3-yl)-6-methoxy-9*H*-pyrimido[4,5-*b*]indol-7-yl)-3,5-dimethylisoxazole (22). Method A using *tert*-butyl 6-fluoro-2-methyl-3-(4,4,5,5-tetramethyl-1,3,2-dioxaborolan-2-yl)-1*H*-indole-1-carboxylate: 52% yield. ^{1}H NMR (MeOD-d_4, 300 MHz): 12.04 (NH), 9.16 (s, 1H), 7.62 (s, 1H), 7.34 (dd, J = 9.33,

DOI: 10.1021/acs.jmedchem.7b00193
J. Med. Chem. XXXX, XXX, XXX−XXX

2.16 Hz, 1H), 7.27 (dd, J = 8.74, 5.06 Hz, 1H), 7.01 (ddd, J = 3.42 (s, 3H), 2.67 (s, 3H), 2.33 (s, 3H), 2.14 (s, 3H). ^{13}C NMR (MeOD-d_4, 75 MHz): 168.2, 161.7 (d, J_{C-F} = 238.7 Hz), 161.1, 157.7, 155.3, 149.3, 148.7, 141.5, 138.0 (d, J_{C-F} = 12.8 Hz), 135.5, 123.7, 123.2, 121.8 (d, J_{C-F} = 9.8 Hz), 121.5, 116.7, 114.6, 113.4, 110.7 (d, J_{C-F} = 24.9 Hz), 106.8, 105.1, 99.6 (d, J_{C-F} = 26.4 Hz), 55.8, 13.0, 11.7, 10.8. ESI-MS calculated for $C_{25}H_{21}FN_5O_2$ $[M + H]^+$ = 442.17. Obtained: 442.50.

4-(6-Methoxy-4-(2-methyl-1*H*-pyrrolo[2,3-*c*]pyridin-3-yl)-9*H*-pyrimido[4,5-*b*]indol-7-yl)-3,5-dimethylisoxazole (23). Method A using *tert*-butyl 2-methyl-3-(4,4,5,5-tetramethyl-1,3,2-dioxaborolan-2-yl)-1*H*-pyrrolo[2,3-c]pyridine-1-carboxylate: 61% yield. ^{1}H NMR (MeOD-d_4, 300 MHz): 9.28 (s, 1H), 9.24 (s, 1H), 8.37 (d, J = 6.53 Hz, 1H), 7.87 (d, J = 6.53 Hz, 1H), 7.63 (s, 1H), 6.77 (s, 1H), 3.47 (s, 3H), 2.85 (s, 3H), 2.32 (s, 3H), 2.14 (s, 3H) ESI-MS calculated for $C_{24}H_{21}N_6O_2$ $[M + H]^+$ = 425.17. Obtained: 425.50.

4-(6-Methoxy-4-(2-methylbenzofuran-3-yl)-9*H*-pyrimido-[4,5-*b*]indol-7-yl)-3,5-dimethylisoxazole (24). Method A using 4,4,5,5-tetramethyl-2-(2-methylbenzofuran-3-yl)-1,3,2-dioxaborolane: 31% yield. ^{1}H NMR (MeOD-d_4, 300 MHz): 9.22 (s, 1H), 7.73 (d, J = 8.32 Hz, 1H), 7.60 (s, 1H), 7.55−7.45 (m, 1H), 7.40−7.30 (m, 2H), 6.85 (s, 1H), 3.37 (s, 3H), 2.68 (s, 3H), 2.30 (s, 3H), 2.12 (s, 3H), ESI-MS calculated for $C_{25}H_{21}N_4O_3$ $[M + H]^+$ = 425.16. Obtained: 425.50.

4-(4-(1*H*-Benzo[*d*]imidazol-1-yl)-6-methoxy-9*H*-pyrimido-[4,5-*b*]indol-7-yl)-3,5-dimethylisoxazole (25). 7 (20 mg, 0.06 mmol), benzimidazole (72 mg, 0.6 mmol), and EtN(*i*-Pr)$_2$ (0.1 mL) were dissolved in anhydrous DMSO (4 mL). The solution was heated at 170 °C for 16 h. HPLC purification of the reaction mixture provided **25** in 32% yield. ^{1}H NMR (MeOD-d_4, 300 MHz): 9.45 (s, 1H), 9.01 (s, 1H), 8.00 (d, J = 8.09 Hz, 1H), 7.67−7.51 (m, 3H), 7.51 (s, 1H), 6.78 (s, 1H), 3.44 (s, 3H), 2.31 (s, 3H), 2.12 (s, 3H). ESI-MS calculated for $C_{23}H_{19}N_6O_2$ $[M + H]^+$ = 411.16. Found: 411.75.

4-(8-Methoxy-1-(pyrazolo[1,5-*a*]pyridin-3-yl)-5*H*-pyrido[4,3-*b*]indol-7-yl)-3,5-dimethylisoxazole (26). Method A using pyrazolo[1,5-*a*]pyridin-3-ylboronic acid pinacol ester: 29% yield. ^{1}H NMR (MeOD-d_4, 300 MHz): 9.05 (s, 1H), 8.89 (d, J = 7.00 Hz, 1H), 8.76 (s, 1H), 7.76 (d, J = 7.85 Hz, 1H), 7.66−7.58 (m, 1H), 7.56 (s, 1H), 7.25 (dd, J = 6.89, 6.92 Hz, 1H), 7.19 (s, 1H),3.60 (s, 3H), 2.32 (s, 3H), 2.14 (s, 3H). ESI-MS calculated for $C_{24}H_{20}N_5O_2$ $[M + H]^+$ = 410.16. Obtained: 410.12.

4-(6-Methoxy-4-(1-methyl-1*H*-indazol-3-yl)-9*H*-pyrimido-[4,5-*b*]indol-7-yl)-3,5-dimethylisoxazole (27). Optimized Suzuki coupling conditions[37] were used to synthesize **27**. 7 (34 mg, 0.1 mmol), 1-methyl-3-(4,4,5,5-tetramethyl-1,3,2-dioxaborolan-2-yl)-1*H*-indazole (75 mg, 0.3 mmol), and Na_2CO_3 (2 M aqueous solution, 50 mg) were mixed in round-bottom flask. To this flask, MeOH (4 mL), PhMe (4 mL), and water (1 mL) were added, and the system was degassed and refilled with pure N_2. $Pd(PPh_3)_4$ (20 mg) was then added. The system was degassed and refilled again with pure N_2. The mixture was heated at reflux for 12 h. The aqueous layer was extracted with EtOAc, and the combined organic layers were washed with brine and dried over anhydrous Na_2SO_4. The volatile components were removed on a rotary evaporator, and the residue was purified by reverse phase HPLC. The desired product **27** was isolated as TFA salt in 23% yield. ^{1}H NMR (DMSO-d_6, 300 MHz): 12.36 (s, 1H), 9.31 (s, 1H), 9.05 (s, 1H), 8.82 (d, J = 8.18 Hz, 1H), 7.85 (d, J = 8.48 Hz, 1H), 7.60−7.50 (m, 1H), 7.39 (s, 1H), 7.40−7.32 (m, 1H), 4.36 (s, 3H), 4.00 (s, 3H), 3.37 (s, NH), 2.32 (s, 3H), 2.13 (s, 3H). ^{13}C NMR (DMSO-d_6, 75 MHz): 165.7, 159.3, 156.9, 153.9, 152.9, 151.7, 141.0, 132.8, 127.0, 123.8, 123.1, 122.4, 119.9, 119.0, 113.4, 110.4, 109.3, 108.1, 55.5, 36.3, 11.4, 10.5. ESI-MS calculated for $C_{24}H_{21}N_6O_2$ $[M + H]^+$ = 425.17. Found: 425.83.

4-(4-(1*H*-Benzo[*d*][1,2,3]triazol-1-yl)-6-methoxy-9*H*-pyrimido[4,5-*b*]indol-7-yl)-3,5-dimethylisoxazole (28). A modified reported method was followed.[42] 7 (34 mg, 0.1 mmol), benzotriazole (14 mg, 0.12 mmol), and K_3PO_4 (42 mg, 0.2 mmol) were added into a round-bottom flask. The round-bottom flask was degassed and refilled with pure N_2 gas. In a second round-bottom flask, $Pd_2(dba)_3$ (9 mg, 0.01 mmol) and (±)-BINAP (15 mg, 0.024 mmol) were added. The round-bottom flask was degassed and refilled with pure N_2. To this flask, anhydrous toluene (10 mL) was added and the solution was heated at 120 °C for 3 min to generate the active catalyst. The active catalyst was transferred into the first flask, and the reaction mixture was heat at reflux for 12 h. The mixture was then diluted with EtOAc and washed with water and brine. The organic layer was collected, the volatile components were removed on a rotary evaporator, and the residue was purified by reverse phase HPLC. The desired product **28** was isolated as a TFA salt in 29% yield. ^{1}H NMR (DMSO-d_6, 300 MHz): 12.88 (s, 1H), 9.04 (s, 1H), 8.61 (s, 1H), 8.26−8.18 (m, 2H), 7.68−7.60 (m, 2H), 7.48 (s, 1H), 3.87 (s, 3H), 3.30 (s, 3H), 3.15 (s, NH), 2.31 (s, 3H), 2.11 (s, 3H). ^{13}C NMR (DMSO-d_6, 75 MHz): 167.6, 160.8, 160.3, 155.3, 153.8, 146.7, 135.3, 130.8, 122.3, 120.5, 119.3, 119.0, 115.9, 114.8, 109.0, 105.8, 57.0, 13.1, 12.1. ESI-MS Calculated for $C_{22}H_{18}N_7O_2$ $[M + H]^+$ = 412.15. Found: 412.42.

4-(6-Methoxy-2-methyl-4-(2-methyl-1*H*-indol-3-yl)-9*H*-pyrimido[4,5-*b*]indol-7-yl)-3,5-dimethylisoxazole (29). Method A using **S10** and *tert*-butyl 2-methyl-3-(4,4,5,5-tetramethyl-1,3,2-dioxaborolan-2-yl)-1*H*-indole-1-carboxylate afforded a mixture of **29** and a Boc group protected **29**. Treatment of the crude mixture with TFA in DCM followed by HPLC purification yield **29** in 27% yield. ^{1}H NMR (MeOD-d_4, 300 MHz): 11.94 (NH), 7.62 (d, J = 8.13 Hz, 1H), 7.57 (s, 1H), 7.35 (ddd, J = 8.17, 6.82, 1.30, 1H), 7.32−7.18 (m, 2H), 6.80 (s, 1H), 3.00 (s, 3H), 2.70 (s, 3H), 2.34 (s, 3H), 2.15 (s, 3H). ^{13}C NMR (MeOD-d_4, 75 MHz):168.1, 161.1, 160.1, 158.2, 155.3, 148.8, 141.0, 137.8, 135.5, 127.2, 124.3, 122.7, 122.5, 121.6, 120.7, 116.6, 114.6, 113.4, 111.7, 107.0, 104.5, 55.8, 22.4, 12.9, 11.7, 10.8. ESI-MS calculated for $C_{26}H_{24}N_5O_2$ $[M + H]^+$ = 438.19. Obtained: 438.42.

Method I: Synthesis of 4-(6-Methoxy-2-methyl-4-(2-methylquinolin-4-yl)-9*H*-pyrimido[4,5-*b*]indol-7-yl)-3,5-dimethylisoxazole (30). For Suzuki coupling catalyzed by $Pd(dppf)Cl_2$−CH_2Cl_2 complex: **S10** (728 mg, 2.1 mmol, 1.0 equiv) and 2-methyl-4-(4,4,5,5-tetramethyl-1,3,2-dioxaborolan-2-yl)quinoline (1.674g, 6.22 mmol, 3.0 equiv) were placed in a round-bottom flask. DME (60 mL) and Na_2CO_3 (2 M aq solution, 20 mL) were added subsequently. The system was degassed to remove oxygen. $Pd(dppf)Cl_2$−CH_2Cl_2 complex (257 mg, 0.31 mmol, >0.1 equiv) was added in one portion. The system was degassed again and refilled with N_2. The reaction was heated at reflux for 16 h before quenching with H_2O. The reaction was then diluted with H_2O, the aqueous layer was extracted with EtOAc (100 mL × 3), and the combined organic layers were dried over anhydrous sodium sulfate. The solvent was removed in vacuum and the residue was purified by flash column chromatography to yield **30** in 0.64 g (63% yield). Further purification was aided by reverse phase HPLC to yield the corresponding products **30** as a salt of CF_3CO_2H. ^{1}H NMR (300 MHz, MeOD-d_4): 8.32 (d, J = 8.47 Hz, 1H), 8.13 (s, 1H), 8.10 (ddd, J = 8.44, 7.03, 1.26 Hz, 1H), 7.93 (d, J = 7.86 Hz, 1H), 7.75 (t, J = 7.71 Hz, 1H), 7.49 (s, 1H), 6.30 (s, 1H), 3.25 (s, 3H), 3.04 (s, 3H), 2.95 (s, 3H), 2.26 (s, 3H), 2.07 (s, 3H). ESI-MS calculated for $C_{27}H_{24}N_5O_2$ $[M + H]^+$ = 450.19. Obtained: 450.42

4-(6-Methoxy-2-methyl-4-(quinolin-4-yl)-9*H*-pyrimido[4,5-*b*]indol-7-yl)-3,5-dimethylisoxazole (31). Method A using **S10** and quinoline-4-boronic acid: 57% yield. ^{1}H NMR (MeOD-d_4, 300 MHz): 9.31 (d, J = 4.59 Hz, 1H), 8.38 (d, J = 8.50 Hz, 1H), 8.08 (d, J = 4.63 Hz, 1H), 8.12−8.00 (m, 1H), 7.88 (d, J = 7.76 Hz, 1H), 7.78−7.70 (m, 1H), 7.53 (s, 1H), 6.21 (s, 1H), 3.21 (s, 3H), 3.00 (s, 3H), 2.26 (s, 3H), 2.07 (s, 3H). ^{13}C NMR (MeOD-d_4, 75 MHz): 168.2, 162.1, 161.0, 158.6, 155.3, 151.0, 150.3, 148.3, 141.3, 136.1, 133.3, 130.8, 129.9, 126.7, 126.2, 123.7, 123.6, 120.4, 117.0, 114.5, 112.9, 105.3, 55.9, 23.6, 11.6, 10.7. ESI-MS calculated for $C_{26}H_{22}N_5O_2$ $[M + H]^+$ = 436.18. Found: 436.50.

4-(6-Methoxy-2-methyl-4-(quinolin-5-yl)-9*H*-pyrimido[4,5-*b*]indol-7-yl)-3,5-dimethylisoxazole (32). Method A using **S10** and quinoline-5-boronic acid: 27%. ^{1}H NMR (300 MHz, MeOD-d_4): 9.15 (dd, J = 4.39, 1.39 Hz, 1H), 8.61−8.53 (m, 1H), 8.41 (d, J = 8.60 Hz, 1H), 8.25 (d, J = 1.33 Hz, 1H), 8.24 (s, 1H), 7.72 (dd, J = 7.74, 4.42 Hz, 1H), 7.57 (s, 1H), 6.30 (s, 1H), 3.28 (s, 3H), 3.03 (3H), 2.29 (s, 3H), 2.10 (s, 3H). ESI-MS calculated for $C_{26}H_{22}N_5O_2$ $[M + H]^+$ = 436.18. Obtained: 436.33.

4-(6-Methoxy-2-methyl-4-(6-methylquinolin-5-yl)-9*H*-pyrimido[4,5-*b*]indol-7-yl)-3,5-dimethylisoxazole (33). Method A using **S10** and 3-methylquinoline-4-boronic acid: 36%. ^{1}H NMR (300 MHz, MeOD-d_4): 9.08 (d, J = 4.56 Hz, 1H), 8.46 (J = 8.81 Hz, 1H), 8.22 (d, J = 8.56 Hz, 1H), 8.17 (d, J = 8.86 Hz, 1H), 7.69 (dd, J = 8.63,

DOI: 10.1021/acs.jmedchem.7b00193
J. Med. Chem. XXXX, XXX, XXX−XXX

4.64 Hz, 1H), 7.55 (s, 1H), 6.14 (s, 1H), 3.28 (s, 3H), 3.01 (s, 3H), 2.47 (s, 3H), 2.25 (s, 3H), 2.06 (s, 3H). ESI-MS calculated for $C_{27}H_{24}N_5O_2$ $[M + H]^+$ = 450.19. Obtained: 450.50.

4-(4-(Isoquinolin-4-yl)-6-methoxy-2-methyl-9*H*-pyrimido-[4,5-*b*]indol-7-yl)-3,5-dimethylisoxazole (34). Method A using **S10** and isoquinoline-4-boronic acid: 54%. ^{1}H NMR (300 MHz, MeOD-d_4): 9.78 (s, 1H), 8.98 (s, 1H), 8.53−8.46 (m, 1H), 8.04−7.92 (m, 2H), 7.90−7.82 (m, 1H), 7.55 (s, 1H), 6.23 (s, 1H), 3.20 (s, 3H), 3.01 (s, 3H), 2.26 (s, 3H), 2.07 (s, 3H). ESI-MS calculated for $C_{26}H_{22}N_5O_2$ $[M + H]^+$ = 436.18. Obtained: 436.50.

4-(4-(Isoquinolin-5-yl)-6-methoxy-2-methyl-9*H*-pyrimido-[4,5-*b*]indol-7-yl)-3,5-dimethylisoxazole (35). Method A using **S10** and isoquinoline-5-boronic acid: 29%. ^{1}H NMR (300 MHz, MeOD-d_4): 9.85 (s, broad, 1H), 8.80 (d, J = 8.32 Hz, 1H), 8.75−8.50 (broad, 1H), 8.56 (dd, J = 7.24, 1.11 Hz), 8.26 (dd, J = 8.29, 7.30 Hz, 1H), 8.04 (d, J = 6.08 Hz, 1H), 6.32 (s, 1H), 3.29 (s, 3H), 3.00 (s, 3H), 2.27 (s, 3H), 2.08 (s, 3H). ^{13}C NMR (75 MHz, MeOD-d_4): 168.1, 162.2, 161.0, 158.7, 155.2, 153.2, 151.8, 141.8, 136.6, 136.0, 135.6, 134.1, 130.6, 130.1, 123.4, 121.1, 120.7, 112.0, 114.5, 113.1, 105.1, 55.9, 23.6, 11.6, 10.7. ESI-MS calculated for $C26H_{22}N_5O_2$ $[M + H]^+$ = 436.18. Obtained: 436.68.

4-(4-(Isoquinolin-8-yl)-6-methoxy-2-methyl-9*H*-pyrimido-[4,5-*b*]indol-7-yl)-3,5-dimethylisoxazole (36). Method A using **S10** and isoquinoline-8-boronic acid: 35%. ^{1}H NMR (300 MHz, MeOD-d_4): 9.54 (s, 1H), 8.74 (s, 1H), 8.61 (dd, J = 7.75, 1.22 Hz, 1H), 8.52 (d, J = 6.18 Hz, 1H), 8.47−8.35 (m, 2H), 7.54 (s, 1H), 6.42 (s, 1H), 3.32 (s, 3H), 2.99 (s, 3H), 2.26 (s, 3H), 2.08 (s, 3H). ^{13}C NMR (75 MHz, MeOD-d_4): 168.1, 162.8, 161.1, 158.8, 155.1, 152.5, 149.7, 140.6, 139.4, 135.9, 134.2, 133.6, 132.8, 132.0, 126.8, 125.0, 123.2, 120.7, 116.9, 114.6, 113.1, 104.9, 56.0, 24.1, 11.6, 10.7. ESI-MS calculated for $C_{26}H_{22}N_5O_2$ $[M + H]^+$ = 436.18. Obtained: 436.56.

4-(6-Methoxy-2-methyl-4-(quinolin-8-yl)-9*H*-pyrimido[4,5-*b*]indol-7-yl)-3,5-dimethylisoxazole (37). Method A using **S10** and quinoline-8-boronic acid: 18%. ^{1}H NMR (300 MHz, MeOD-d_4): 8.89 (dd, J = 4.28, 1.72 Hz, 1H), 8.65 (dd, J = 8.41, 1.68 Hz, 1H), 8.47 (dd, J = 8.28, 1.31 Hz, 1H), 8.37 (dd, J = 7.18, 1.36 Hz, 1H), 8.02 (dd, J = 8.20, 7.26 Hz, 1H), 7.74 (dd, J = 8.38, 4.28 Hz, 1H), 7.54 (s, 1H), 6.43 (s, 1H), 3.33 (s, 3H), 2.99 (s, 3H), 2.27 (s, 3H), 2.08 (s, 3H). ESI-MS calculated for $C_{26}H_{22}N_5O_2$ $[M + H]^+$ = 436.18. Obtained: 436.83.

4-(6-Methoxy-2-methyl-4-(2-(trifluoromethyl)quinolin-4-yl)-9*H*-pyrimido[4,5-*b*]indol-7-yl)-3,5-dimethylisoxazole (38). Method I using **S10** and 4-(4,4,5,5-tetramethyl-1,3,2-dioxaborolan-2-yl)-2-(trifluoromethyl)quinoline: 10% yield. ^{1}H NMR (300 MHz, MeOD-d_4): 8.44 (d, J = 8.61 Hz, 1H), 8.28 (s, 1H), 8.04 (t, J = 7.71 Hz, 1H), 7.90 (d, J = 8.19 Hz, 1H), 7.76 (t, J = 8.03 Hz, 1H), 7.45 (s, 1H), 6.20 (s, 1H), 3.21 (s, 3H), 2.93 (s, 3H), 2.26 (s, 3H), 2.07 (s, 3H). ESI-MS calculated for $C_{27}H_{21}F_3N_5O_2$ $[M + H]^+$ = 504.16. Obtained: 504.58.

4-(6-Methoxy-4-(2-methoxyquinolin-4-yl)-2-methyl-9*H*-pyrimido[4,5-*b*]indol-7-yl)-3,5-dimethylisoxazole (39). Method I using **S10** and 2-methoxy-4-(4,4,5,5-tetramethyl-1,3,2-dioxaborolan-2-yl)quinoline: 35% yield. ^{1}H NMR (300 MHz, MeOD-d_4): 8.11 (d, J = 8.44 Hz, 1H), 7.83 (ddd, J = 8.39, 7.05, 1.30 Hz, 1H), 7.63 (d, J = 8.29 Hz, 1H), 7.54 (s, 1H), 7.49 (s, 1H), 7.44 (t, J = 7.63 Hz, 1H), 6.27 (s, 1H), 4.20 (s, 3H), 3.21 (s, 3H), 3.00 (s, 3H), 2.26 (s, 3H), 2.07 (s, 3H). ESI-MS calculated for $C_{27}H_{24}N_5O_3$ $[M + H]^+$ = 466.19. Obtained: 466.68.

4-(6-Methoxy-2-methyl-4-(quinolin-3-yl)-9*H*-pyrimido[4,5-*b*]indol-7-yl)-3,5-dimethylisoxazole (40). Method A using **S10** and quinoline-3-boronic acid: 22% yield. ^{1}H NMR (300 MHz, MeOD-d_4): 9.47 (d, J = 2.01 Hz, 1H), 9.21 (d, J = 2.03 Hz, 1H), 8.29 (t, J = 7.52 Hz, 2H), 8.08 (ddd, J = 8.50, 6.99, 1.40 Hz, 1H), 7.88 (ddd, J = 8.05, 7.14, 1.00 Hz, 1H), 7.57 (s,1H), 7.29 (s, 1H), 3.60 (s, 3H), 3.00 (s, 3H), 2.31 (s, 3H), 2.13 (s, 3H). ESI-MS calculated for $C_{26}H_{22}N_5O_2$ $[M + H]^+$ = 436.18. Obtained: 436.83.

The procedures for FP-based protein binding assay, cell growth inhibition assay, and Western blotting have been reported in our previous paper (see that paper for experimental details).[33]

Determination of Biochemical Binding Affinities to BET Proteins. Recombinant human proteins corresponding to BRD2 BD1 (residues 72−205), BRD2 BD2 (residues 349−460), BRD3 BD1 (residues 24−144), BRD3 BD2 (residues 306−417), BRD4 BD1 (residues 44−168), BRD4 BD2 (residues 333−460) were used in the biochemical binding assays. Binding affinities of BET inhibitors to BRD2 (BD1 and BD2 proteins), BRD3 (BD1 and BD2 proteins), BRD4 (BD1 and BD2 proteins) were determined using our established fluorescence-polarization binding assays as described previously.[33]

Determination of the Cocrystal Structure of Compound 31 in Complex with BRD4 BD2 Protein. Prior to crystallization, BRD4 BD2 concentrated to 7.1 mg/mL in 25 mM Tris-HCl, pH 7.5, 150 mM NaCl, and 1 mM TCEP was incubated with a 2-fold molar excess of compound **31** for 1 h and then incubated with 0.5% β-mercaptoethanol for an additional 2 h at room temperature. Crystals were grown at 20 °C from drops containing equal volumes of protein complex and well solution (50% polyethylene glycol 400, 10 mM imidazole, pH 8.0, and 0.5 mM ATP). For data collection, the crystals were mounted directly from the drop and flash frozen in liquid nitrogen. Data were collected at the Advance Photon Source at Argonne National Lab on the LS-CAT beamlines 21-ID-G. The complex crystallized in space group $P2_12_12$ and contained 1 molecule per asymmetric unit. Data were processed with HKL2000,[43] and the structure was solved by molecular replacement with Phaser[44] using an in-house structure as a model. The structure was refined with BUSTER,[45] and electron density maps were fit with COOT.[46] Coordinates and restraints for the compounds were developed using grade with the mogul+qm option.[45] Structures were validated using Molprobity.[47] Ligand statistics were obtained from the wwPDB validation server. Data refinement and statistics are given in Supporting Information Table S1. The coordinates were deposited in the PDB with the following identifier: 5UOO.

Cell Growth Inhibition and Western Blotting. The SUM-149PT human breast cancer cell line was developed at the University of Michigan Comprehensive Cancer Center.[48] All the other human cancer cell lines were purchased from the American Type Culture Collection. Cells were used within 1 month after thaw and were cultured as recommended.

In cell growth assay, cells were seeded in 96-well cell culture plates at 10 000 cells/well for leukemia cells and 3000 cells/well for breast cancer cells in 75 μL of culture medium. Compounds were serially diluted in culture medium, and 75 μL of the diluted compounds was added to the plates. The cells were then cultured for 4 days. Cell growth was evaluated by the dehydrogenases-based WST-8 assay (Dojindo Molecular Technologies). The WST-8 reagent was added to the plate at a final concentration of 10% (v/v), incubated for 1−3 h, and read at 450 nm using a Tecan Infinite M1000 multimode microplate reader (Tecan, Morrisville, NC). The readings were normalized to the DMSO-treated cells, and the IC_{50} was calculated by nonlinear regression analysis using GraphPad Prism 6 software.

For Western blot analysis, cells were treated with compounds at indicated conditions. Cells were collected and lysed in RIPA buffer containing protease inhibitors. Whole cell lysates were separated by 4−20% SDS−PAGE gels and blotted into PVDF membranes. For immunoblotting, rabbit polyclonal antibodies for BRD2, BRD3, and BRD4 were from Bethyl Laboratories (Montgomery, TX, USA), mouse monoclonal antibody for c-Myc was from Cell Signaling Technology (Danvers, MA, USA), and GAPDH was from Santa Cruz Biotechnologies (Dallas, TX, USA).

Microsomal Stability Studies. The metabolic stability was assessed using pooled CD-1 mouse liver microsomes, pooled SD rat liver microsmes, and pooled human liver microsome (purchased from Xeno Tech). Briefly, 1 μM of each compound (**21**, **29**, **30**, and **31**) was incubated with 0.5 mg/mL microsomes and 1.7 mM cofactor β-NADPH in 0.1 M phosphate buffer (pH = 7.4) containing 3.3 mM $MgCl_2$ at 37 °C. The DMSO concentration was less than 0.1% in the final incubation system. At 5, 10, 15, 30, 45, and 60 min of incubation, an amount of 40 μL of reaction mixture was taken out, and the reaction is stopped immediately by adding 3-fold excess of cold acetonitrile containing 100 ng/mL of internal standard for quantification. The collected fractions were centrifuged at 15 000 rpm for 10 min to collect the supernatant for LC−MS/MS analysis, from which the amount of compound remaining was determined. The natural log of the amount of compound remaining was plotted against time to determine the disappearance rate and the half-life of tested compounds.

DOI: 10.1021/acs.jmedchem.7b00193
J. Med. Chem. XXXX, XXX, XXX−XXX

Pharmacokinetic Studies in Rats and Mice. All animal experiments were approved by the University of Michigan Committee on Use and Care of Animals and Unit for Laboratory Animal Medicine under the approved protocol (PRO00005315, P.I. Shaomeng Wang).

The pharmacokinetics of compounds **21** and **31** was determined in Sprague Dawley rats following intravenous (iv) dosing at 5 mg/kg or oral (po) dosing at 25 mg/kg. The quick pharmacokinetics of compound **17** was determined in SCID mice following po dosing at 25 mg/kg.

A tested compound was dissolved in the vehicle containing 20% (v/v) PCP and 70% (v/v) PBS. Blood samples (100 μL) were collected from rats with a catheter at different time points (0, 5 min, 15 min, 30 min, 1 h, 2 h, 4 h, 6 h, 8 h, and 24 h) after the treatment of drugs. The blood samples were centrifuged at 15 000 rpm for 10 min, then the supernatant plasma was saved at −80 °C until analysis.

Plasma concentrations of the compounds were determined by the LC−MS/MS method developed and validated for this study. The LC−MS/MS method consisted of a Shimadzu HPLC system, and chromatographic separation of tested compound was achieved using a Waters XBridge-C18 column (5 cm × 2.1 mm, 3.5 μm). An AB Sciex QTrap 4500 mass spectrometer equipped with an electrospray ionization source (Applied Biosystems, Toronto, Canada) in the positive-ion multiple reaction monitoring (MRM) mode was used for detection. The mobile phases were 0.1% formic acid in purified water (A) and 0.1% formic acid in acetonitrile (B). The gradient (B) was held at 10% (0−0.3 min), increased to 95% at 0.7 min, then stayed at isocratic 95% B for 2.3 min, and then immediately stepped back down to 10% for 2 min of re-equilibration. Flow rate was set at 0.4 mL/min. All pharmacokinetic parameters were calculated by noncompartmental methods using WinNonlin, version 3.2 (Pharsight Corporation, Mountain View, CA, USA).

Efficacy Studies in the MV4;11 and MDA-MB-231 Xenograft Models in Mice. All efficacy experiments were done under the guidelines of the University of Michigan Committee for Use and Care of Animals and using an approved animal protocol (PRO00005315, P.I. Shaomeng Wang).

To develop xenograft tumors, 5×10^6 MV4;11 or MDA-MB-231 cells with 50% Matrigel were injected subcutaneously on the dorsal side of severe combined immunodeficient (SCID) mice, obtained from Charles River, one tumor per mouse. When tumors reached ∼100 mm^3, mice were randomly assigned to treatment and vehicle control groups. Animals were monitored daily for any signs of toxicity and weighed 2−3 times per week during the treatment and weighed at least weekly after the treatment was ended. Tumor size was measured 2−3 times per week by electronic calipers during the treatment period and at least weekly after the treatment was ended. Tumor volume was calculated as $V = L \times W^2/2$, where L is the length and W is the width of the tumor.

■ ASSOCIATED CONTENT

Supporting Information

The Supporting Information is available free of charge on the ACS Publications website at DOI: 10.1021/acs.jmedchem.7b00193.

Crystallography data collection and refinement statistics (PDF)

Molecular formula strings and some data (CSV)

Accession Codes

Atomic coordinates have been deposited in the Protein Data Bank (PDB code 5UOO for **31**). Authors will release the atomic coordinates and experimental data upon article publication.

■ AUTHOR INFORMATION

Corresponding Author

*Phone: 734-6150362. Fax: 734-6479647. E-mail: shaomeng@umich.edu.

ORCID

Chao-Yie Yang: 0000-0002-5445-0109

Bing Zhou: 0000-0003-1813-8035

Shaomeng Wang: 0000-0002-8782-6950

Present Addresses

[‖]Y.Z. and B.Z.: State Key Laboratory of Drug Research, Shanghai Institute of Materia Medica, Chinese Academy of Sciences, Shanghai 201203, China.

[⊥]X.R.: Institute for Neurodegenerative Diseases, University of California, San Francisco 94143, United States.

Notes

The authors declare the following competing financial interest(s): Multiple patents have been filed by University of Michigan on this class of BET bromodomain in inhibitors, which have been licensed by OncoFusion Therapeutics Inc. Shaomeng Wang, Yujun Zhao, Xu Ran, Liu Liu, Longchuan Bai, Chao-Yie Yang, Bo Wen, Ting Zhao, Duxin Sun, Donna McEachern, and Xiaoqin Li are inventors of the BET bromodomain inhibitors reported in this manuscript and receive royalties from University of Michigan. Shaomeng Wang also owns stock in and serves as a consultant for OncoFusion Therapeutics Inc. The University of Michigan and Shaomeng Wang have also received a research contract from OncoFusion Therapeutics Inc.

■ ACKNOWLEDGMENTS

This study is supported in part by the Prostate Cancer Foundation, OncoFusion Therapeutics, the University of Michigan Comprehensive Cancer Core grant (NIH/NCI, Grant P30CA046592), and the University of Michigan Prostate Cancer SPORE grant (NIH/NCI, Grant P50 CA186786). Use of the Advanced Photon Source, an Office of Science User Facility operated for the U.S. Department of Energy (DOE) Office of Science by Argonne National Laboratory, was supported by the U.S. DOE under Contract DE-AC02-06CH11357. The Life Sciences Collaborative Access Team (LS-CAT) at Sector 21 of the Advanced Photon Source at Argonne National Laboratory was supported by the Michigan Economic Development Corporation and the Michigan Technology Tri-Corridor (Grant 085P1000817). We thank Dr. David Smith of LS-CAT for his assistance with crystal screening and remote data collection. The content is solely the responsibility of the authors and does not necessarily represent the official views of the National Institutes of Health or other funding agencies.

■ ABBREVIATIONS USED

DME, 1,2-dimethoxyethane; DMF, dimethylformamide; NMP, 1-methylpyrrolidin-2-one; C_{max}, peak plasma concentration of a drug after administration; V_{ss}, apparent volume in which a drug is distributed at steady state; CL, volume of plasma cleared of the drug per unit time; PARP, poly (ADP-ribose) polymerase; CL-PARP, cleaved poly (ADP-ribose) polymerase

■ REFERENCES

(1) Arrowsmith, C. H.; Bountra, C.; Fish, P. V.; Lee, K.; Schapira, M. Epigenetic protein families: a new frontier for drug discovery. *Nat. Rev. Drug Discovery* **2012**, *11*, 384−400.

(2) Belkina, A. C.; Denis, G. V. BET domain co-regulators in obesity, inflammation and cancer. *Nat. Rev. Cancer* **2012**, *12*, 465−477.

(3) Filippakopoulos, P.; Qi, J.; Picaud, S.; Shen, Y.; Smith, W. B.; Fedorov, O.; Morse, E. M.; Keates, T.; Hickman, T. T.; Felletar, I.; Philpott, M.; Munro, S.; McKeown, M. R.; Wang, Y.; Christie, A. L.; West, N.; Cameron, M. J.; Schwartz, B.; Heightman, T. D.; La Thangue, N.; French, C. A.; Wiest, O.; Kung, A. L.; Knapp, S.; Bradner, J. E. Selective inhibition of BET bromodomains. *Nature* **2010**, *468*, 1067−1073.

DOI: 10.1021/acs.jmedchem.7b00193
J. Med. Chem. XXXX, XXX, XXX−XXX

(4) Dawson, M. A.; Prinjha, R. K.; Dittmann, A.; Giotopoulos, G.; Bantscheff, M.; Chan, W. I.; Robson, S. C.; Chung, C. W.; Hopf, C.; Savitski, M. M.; Huthmacher, C.; Gudgin, E.; Lugo, D.; Beinke, S.; Chapman, T. D.; Roberts, E. J.; Soden, P. E.; Auger, K. R.; Mirguet, O.; Doehner, K.; Delwel, R.; Burnett, A. K.; Jeffrey, P.; Drewes, G.; Lee, K.; Huntly, B. J.; Kouzarides, T. Inhibition of BET recruitment to chromatin as an effective treatment for MLL-fusion leukaemia. *Nature* **2011**, *478*, 529−533.

(5) Nicodeme, E.; Jeffrey, K. L.; Schaefer, U.; Beinke, S.; Dewell, S.; Chung, C. W.; Chandwani, R.; Marazzi, I.; Wilson, P.; Coste, H.; White, J.; Kirilovsky, J.; Rice, C. M.; Lora, J. M.; Prinjha, R. K.; Lee, K.; Tarakhovsky, A. Suppression of inflammation by a synthetic histone mimic. *Nature* **2010**, *468*, 1119−1123.

(6) Anand, P.; Brown, J. D.; Lin, C. Y.; Qi, J.; Zhang, R.; Artero, P. C.; Alaiti, M. A.; Bullard, J.; Alazem, K.; Margulies, K. B.; Cappola, T. P.; Lemieux, M.; Plutzky, J.; Bradner, J. E.; Haldar, S. M. BET bromodomains mediate transcriptional pause release in heart failure. *Cell* **2013**, *154*, 569−582.

(7) Gosmini, R.; Nguyen, V. L.; Toum, J.; Simon, C.; Brusq, J. M.; Krysa, G.; Mirguet, O.; Riou-Eymard, A. M.; Boursier, E. V.; Trottet, L.; Bamborough, P.; Clark, H.; Chung, C. W.; Cutler, L.; Demont, E. H.; Kaur, R.; Lewis, A. J.; Schilling, M. B.; Soden, P. E.; Taylor, S.; Walker, A. L.; Walker, M. D.; Prinjha, R. K.; Nicodeme, E. The discovery of I-BET726 (GSK1324726A), a potent tetrahydroquinoline ApoA1 up-regulator and selective BET bromodomain inhibitor. *J. Med. Chem.* **2014**, *57*, 8111−8131.

(8) Gehling, V. S.; Hewitt, M. C.; Vaswani, R. G.; Leblanc, Y.; Cote, A.; Nasveschuk, C. G.; Taylor, A. M.; Harmange, J. C.; Audia, J. E.; Pardo, E.; Joshi, S.; Sandy, P.; Mertz, J. A.; Sims, R. J., 3rd; Bergeron, L.; Bryant, B. M.; Bellon, S.; Poy, F.; Jayaram, H.; Sankaranarayanan, R.; Yellapantula, S.; Bangalore Srinivasamurthy, N.; Birudukota, S.; Albrecht, B. K. Discovery, design, and optimization of isoxazole azepine BET inhibitors. *ACS Med. Chem. Lett.* **2013**, *4*, 835−840.

(9) Wong, C.; Laddha, S. V.; Tang, L.; Vosburgh, E.; Levine, A. J.; Normant, E.; Sandy, P.; Harris, C. R.; Chan, C. S.; Xu, E. Y. The bromodomain and extra-terminal inhibitor CPI203 enhances the antiproliferative effects of rapamycin on human neuroendocrine tumors. *Cell Death Dis.* **2014**, *5*, e1450−e1450.

(10) Fish, P. V.; Filippakopoulos, P.; Bish, G.; Brennan, P. E.; Bunnage, M. E.; Cook, A. S.; Federov, O.; Gerstenberger, B. S.; Jones, H.; Knapp, S.; Marsden, B.; Nocka, K.; Owen, D. R.; Philpott, M.; Picaud, S.; Primiano, M. J.; Ralph, M. J.; Sciammetta, N.; Trzupek, J. D. Identification of a chemical probe for bromo and extra C-terminal bromodomain inhibition through optimization of a fragment-derived hit. *J. Med. Chem.* **2012**, *55*, 9831−9837.

(11) Bamborough, P.; Diallo, H.; Goodacre, J. D.; Gordon, L.; Lewis, A.; Seal, J. T.; Wilson, D. M.; Woodrow, M. D.; Chung, C. W. Fragment-based discovery of bromodomain inhibitors part 2: optimization of phenylisoxazole sulfonamides. *J. Med. Chem.* **2012**, *55*, 587−596.

(12) McKeown, M. R.; Shaw, D. L.; Fu, H.; Liu, S.; Xu, X.; Marineau, J. J.; Huang, Y.; Zhang, X.; Buckley, D. L.; Kadam, A.; Zhang, Z.; Blacklow, S. C.; Qi, J.; Zhang, W.; Bradner, J. E. Biased multicomponent reactions to develop novel bromodomain inhibitors. *J. Med. Chem.* **2014**, *57*, 9019−9027.

(13) Hewings, D. S.; Fedorov, O.; Filippakopoulos, P.; Martin, S.; Picaud, S.; Tumber, A.; Wells, C.; Olcina, M. M.; Freeman, K.; Gill, A.; Ritchie, A. J.; Sheppard, D. W.; Russell, A. J.; Hammond, E. M.; Knapp, S.; Brennan, P. E.; Conway, S. J. Optimization of 3,5-dimethylisoxazole derivatives as potent bromodomain ligands. *J. Med. Chem.* **2013**, *56*, 3217−3227.

(14) Seal, J.; Lamotte, Y.; Donche, F.; Bouillot, A.; Mirguet, O.; Gellibert, F.; Nicodeme, E.; Krysa, G.; Kirilovsky, J.; Beinke, S.; McCleary, S.; Rioja, I.; Bamborough, P.; Chung, C. W.; Gordon, L.; Lewis, T.; Walker, A. L.; Cutler, L.; Lugo, D.; Wilson, D. M.; Witherington, J.; Lee, K.; Prinjha, R. K. Identification of a novel series of BET family bromodomain inhibitors: binding mode and profile of I-BET151 (GSK1210151A). *Bioorg. Med. Chem. Lett.* **2012**, *22*, 2968−2972.

(15) Mirguet, O.; Lamotte, Y.; Donche, F.; Toum, J.; Gellibert, F.; Bouillot, A.; Gosmini, R.; Nguyen, V. L.; Delannee, D.; Seal, J.; Blandel, F.; Boullay, A. B.; Boursier, E.; Martin, S.; Brusq, J. M.; Krysa, G.; Riou, A.; Tellier, R.; Costaz, A.; Huet, P.; Dudit, Y.; Trottet, L.; Kirilovsky, J.; Nicodeme, E. From ApoA1 upregulation to BET family bromodomain inhibition: discovery of I-BET151. *Bioorg. Med. Chem. Lett.* **2012**, *22*, 2963−2967.

(16) Zhao, L.; Cao, D.; Chen, T.; Wang, Y.; Miao, Z.; Xu, Y.; Chen, W.; Wang, X.; Li, Y.; Du, Z.; Xiong, B.; Li, J.; Xu, C.; Zhang, N.; He, J.; Shen, J. Fragment-based drug discovery of 2-thiazolidinones as inhibitors of the histone reader BRD4 bromodomain. *J. Med. Chem.* **2013**, *56*, 3833−3851.

(17) Hewings, D. S.; Rooney, T. P. C.; Jennings, L. E.; Hay, D. A.; Schofield, C. J.; Brennan, P. E.; Knapp, S.; Conway, S. J. Progress in the development and application of small molecule inhibitors of bromodomain−acetyl-lysine interactions. *J. Med. Chem.* **2012**, *55*, 9393−9413.

(18) Chapuy, B.; McKeown, M. R.; Lin, C. Y.; Monti, S.; Roemer, M. G.; Qi, J.; Rahl, P. B.; Sun, H. H.; Yeda, K. T.; Doench, J. G.; Reichert, E.; Kung, A. L.; Rodig, S. J.; Young, R. A.; Shipp, M. A.; Bradner, J. E. Discovery and characterization of super-enhancer-associated dependencies in diffuse large B cell lymphoma. *Cancer Cell* **2013**, *24*, 777−790.

(19) Wang, S.; Sun, W.; Zhao, Y.; McEachern, D.; Meaux, I.; Barriere, C.; Stuckey, J. A.; Meagher, J. L.; Bai, L.; Liu, L.; Hoffman-Luca, C. G.; Lu, J.; Shangary, S.; Yu, S.; Bernard, D.; Aguilar, A.; Dos-Santos, O.; Besret, L.; Guerif, S.; Pannier, P.; Gorge-Bernat, D.; Debussche, L. SAR405838: An optimized inhibitor of MDM2-p53 interaction that induces complete and durable tumor regression. *Cancer Res.* **2014**, *74*, 5855−5865.

(20) Banerjee, C.; Archin, N.; Michaels, D.; Belkina, A. C.; Denis, G. V.; Bradner, J.; Sebastiani, P.; Margolis, D. M.; Montano, M. BET bromodomain inhibition as a novel strategy for reactivation of HIV-1. *J. Leukocyte Biol.* **2012**, *92*, 1147−1154.

(21) Matzuk, M. M.; McKeown, M. R.; Filippakopoulos, P.; Li, Q.; Ma, L.; Agno, J. E.; Lemieux, M. E.; Picaud, S.; Yu, R. N.; Qi, J.; Knapp, S.; Bradner, J. E. Small-molecule inhibition of BRDT for male contraception. *Cell* **2012**, *150*, 673−684.

(22) Mertz, J. A.; Conery, A. R.; Bryant, B. M.; Sandy, P.; Balasubramanian, S.; Mele, D. A.; Bergeron, L.; Sims, R. J., 3rd Targeting MYC dependence in cancer by inhibiting BET bromodomains. *Proc. Natl. Acad. Sci. U. S. A.* **2011**, *108*, 16669−16674.

(23) Asangani, I. A.; Dommeti, V. L.; Wang, X.; Malik, R.; Cieslik, M.; Yang, R.; Escara-Wilke, J.; Wilder-Romans, K.; Dhanireddy, S.; Engelke, C.; Iyer, M. K.; Jing, X.; Wu, Y. M.; Cao, X.; Qin, Z. S.; Wang, S.; Feng, F. Y.; Chinnaiyan, A. M. Therapeutic targeting of BET bromodomain proteins in castration-resistant prostate cancer. *Nature* **2014**, *510*, 278−282.

(24) Romero, F. A.; Taylor, A. M.; Crawford, T. D.; Tsui, V.; Côté, A.; Magnuson, S. Disrupting acetyl-lysine recognition: progress in the development of bromodomain inhibitors. *J. Med. Chem.* **2016**, *59*, 1271−1298.

(25) Waring, M. J.; Chen, H. W.; Rabow, A. A.; Walker, G.; Bobby, R.; Boiko, S.; Bradbury, R. H.; Callis, R.; Clark, E.; Dale, I.; Daniels, D. L.; Dulak, A.; Flavell, L.; Holdgate, G.; Jowitt, T. A.; Kikhney, A.; McAlister, M.; Mendez, J.; Ogg, D.; Patel, J.; Petteruti, P.; Robb, G. R.; Robers, M. B.; Saif, S.; Stratton, N.; Svergun, D. I.; Wang, W. X.; Whittaker, D.; Wilson, D. M.; Yao, Y. Potent and selective bivalent inhibitors of BET bromodomains. *Nat. Chem. Biol.* **2016**, *12*, 1097−1104.

(26) Bradbury, R. H.; Callis, R.; Carr, G. R.; Chen, H. W.; Clark, E.; Feron, L.; Glossop, S.; Graham, M. A.; Hattersley, M.; Jones, C.; Lamont, S. G.; Ouvry, G.; Patel, A.; Patel, J.; Rabow, A. A.; Roberts, C. A.; Stokes, S.; Stratton, N.; Walker, G. E.; Ward, L.; Whalley, D.; Whittaker, D.; Wrigley, G.; Waring, M. J. Optimization of a series of bivalent triazolopyridazine based bromodomain and extraterminal inhibitors: the discovery of (3R)-4-[2-[4-[1-(3-methoxy-[1,2,4]triazolo-[4,3-b]pyridazin-6-yl)-4-piperidyl]phenoxylethy]-1,3-dimethyl-piperazin-2-one (AZD5153). *J. Med. Chem.* **2016**, *59*, 7801−7817.

(27) Tanaka, M.; Roberts, J. M.; Seo, H. S.; Souza, A.; Paulk, J.; Scott, T. G.; DeAngelo, S. L.; Dhe-Paganon, S.; Bradner, J. E. Design and

DOI: 10.1021/acs.jmedchem.7b00193
J. Med. Chem. XXXX, XXX, XXX−XXX

characterization of bivalent BET inhibitors. *Nat. Chem. Biol.* **2016**, *12*, 1089−1096.
(28) Albrecht, B. K.; Gehling, V. S.; Hewitt, M. C.; Vaswani, R. G.; Côté, A.; Leblanc, Y.; Nasveschuk, C. G.; Bellon, S.; Bergeron, L.; Campbell, R.; Cantone, N.; Cooper, M. R.; Cummings, R. T.; Jayaram, H.; Joshi, S.; Mertz, J. A.; Neiss, A.; Normant, E.; O'Meara, M.; Pardo, E.; Poy, F.; Sandy, P.; Supko, J.; Sims, R. J.; Harmange, J.-C.; Taylor, A. M.; Audia, J. E. Identification of a benzoisoxazoloazepine inhibitor (CPI-0610) of the bromodomain and extra-terminal (BET) family as a candidate for human clinical trials. *J. Med. Chem.* **2016**, *59*, 1330−1339.
(29) Dombret, H.; Preudhomme, C.; Berthon, C.; Raffoux, E.; Thomas, X.; Vey, N.; Gomez-Roca, C.; Ethell, M.; Yee, K.; Bourdel, F.; Herait, P.; Michallet, M.; Recher, C.; Roumier, C.; Quesnel, B. A phase 1 study of the BET-bromodomain inhibitor OTX015 in patients with advanced acute leukemia. *Blood* **2014**, *124*, 117−117.
(30) Stathis, A.; Quesnel, B.; Amorim, S.; Thieblemont, C.; Zucca, E.; Raffoux, E.; Dombret, H.; Peng, Y.; Palumbo, A.; Vey, N.; Thomas, X.; Michallet, M.; Gomez-Roca, C.; Recher, C.; Karlin, L.; Yee, K.; Rezai, K.; Preudhomme, C.; Facon, T.; Herait, R. Results of a first-in-man phase I trial assessing OTX015, an orally available BET-bromodomain (BRD) inhibitor, in advanced hematologic malignancies. *Eur. J. Cancer* **2014**, *50*, 196−196.
(31) Vazquez, R.; Astorgues-Xerri, L.; Riveiro, M. E.; Di Marino, M.; Beltrame, L.; Bekradda, M.; Cvitkovic, E.; Erba, E.; Frapolli, R.; D'Incalci, M. Evaluation of the pan-BET-bromodomain inhibitor OTX015 as a single agent and in combination with everolimus (RAD001) in triple-negative breast cancer. *Eur. J. Cancer* **2014**, *50*, 187−187.
(32) Herait, P. E.; Berthon, C.; Thieblemont, C.; Raffoux, E.; Magarotto, V.; Stathis, A.; Thomas, X.; Leleu, X.; Gomez-Roca, C.; Odore, E.; Roumier, C.; Bourdel, F.; Quesnel, B.; Zucca, E.; Michallet, M.; Recher, C.; Cvitkovic, E.; Rezai, K.; Preudhomme, C.; Facon, T.; Palumbo, A.; Dombret, H. BET-bromodomain inhibitor OTX015 shows clinically meaningful activity at nontoxic doses: interim results of an ongoing phase I trial in hematologic malignancies. *Cancer Res.* **2014**, *74*, CT231.
(33) Ran, X.; Zhao, Y.; Liu, L.; Bai, L.; Yang, C.-Y.; Zhou, B.; Meagher, J. L.; Chinnaswamy, K.; Stuckey, J. A.; Wang, S. Structure-based design of γ-carboline analogues as potent and specific BET bromodomain inhibitors. *J. Med. Chem.* **2015**, *58*, 4927−4939.
(34) https://www.discoverx.com/services/drug-discovery-development-services/epigenetic-profiling/bromoscan (accessed April 12, 2017).
(35) Breslin, H. J.; Lane, B. M.; Ott, G. R.; Ghose, A. K.; Angeles, T. S.; Albom, M. S.; Cheng, M.; Wan, W.; Haltiwanger, R. C.; Wells-Knecht, K. J.; Dorsey, B. D. Design, synthesis, and anaplastic lymphoma kinase (ALK) inhibitory activity for a novel series of 2,4,8,22-tetraazatetracyclo-[14.3.1.1^{3,7}.1^{9,13}]docosa-1(20),3(22),4,6,9(21),10,12,16,18-nonaene macrocycles. *J. Med. Chem.* **2012**, *55*, 449−464.
(36) Showalter, H. D.; Bridges, A. J.; Zhou, H.; Sercel, A. D.; McMichael, A.; Fry, D. W. Tyrosine kinase inhibitors. 16. 6,5,6-tricyclic benzothieno[3, 2-d]pyrimidines and pyrimido[5,4-b-] and -[4,5-b]-indoles as potent inhibitors of the epidermal growth factor receptor tyrosine kinase. *J. Med. Chem.* **1999**, *42*, 5464−5474.
(37) Jimenez, J. M.; Boyall, D.; Brenchley, G.; Collier, P. N.; Davis, C. J.; Fraysse, D.; Keily, S. B.; Henderson, J.; Miller, A.; Pierard, F.; Settimo, L.; Twin, H. C.; Bolton, C. M.; Curnock, A. P.; Chiu, P.; Tanner, A. J.; Young, S. Design and optimization of selective protein kinase C theta (PKCtheta) inhibitors for the treatment of autoimmune diseases. *J. Med. Chem.* **2013**, *56*, 1799−1810.
(38) Li, W.; Nelson, D. P.; Jensen, M. S.; Hoerrner, R. S.; Cai, D.; Larsen, R. D.; Reider, P. J. An improved protocol for the preparation of 3-pyridyl- and some arylboronic acids. *J. Org. Chem.* **2002**, *67*, 5394−5397.
(39) Lefoix, M.; Daillant, J. P.; Routier, S.; Merour, J. Y.; Gillaizeau, I.; Coudert, G. Versatile and convenient methods for the synthesis of C-2 and C-3 functionalised 5-azaindoles. *Synthesis* **2005**, *2005*, 3581−3588.
(40) de Koning, P. D.; McAndrew, D.; Moore, R.; Moses, I. B.; Boyles, D. C.; Kissick, K.; Stanchina, C. L.; Cuthbertson, T.; Kamatani, A.; Rahman, L.; Rodriguez, R.; Urbina, A.; Sandoval, A.; Rose, P. R. Fit-for-purpose development of the enabling route to crizotinib (PF-02341066). *Org. Process Res. Dev.* **2011**, *15*, 1018−1026.
(41) Kruger, A. W.; Rozema, M. J.; Chu-Kung, A.; Gandarilla, J.; Haight, A. R.; Kotecki, B. J.; Richter, S. M.; Schwartz, A. M.; Wang, Z. The discovery and development of a safe, practical synthesis of ABT-869. *Org. Process Res. Dev.* **2009**, *13*, 1419−1425.
(42) Ueda, S.; Ali, S.; Fors, B. P.; Buchwald, S. L. Me$_3$(OMe)-tBuXPhos: A surrogate ligand for Me$_4$tBuXPhos in palladium-catalyzed C−N and C−O bond-forming reactions. *J. Org. Chem.* **2012**, *77*, 2543−2547.
(43) Otwinowski, Z.; Minor, W. Processing of X-ray diffraction data collected in oscillation mode. *Methods Enzymol.* **1997**, *276*, 307−326.
(44) Mccoy, A. J.; Grosse-Kunstleve, R. W.; Adams, P. D.; Winn, M. D.; Storoni, L. C.; Read, R. J. Phaser crystallographic software. *J. Appl. Crystallogr.* **2007**, *40*, 658−674.
(45) Bricogne, G.; Blanc, E.; Brandl, M. T.; Flensburg, C.; Keller, P.; Paciorek, W.; Roversi, P.; Sharff, A.; Smart, O. S.; Vonrhein, C.; Womack, T. O. Grade. *BUSTER*, version 2.10.0; Global Phasing Ltd.; Cambridge, U.K., 2011.
(46) Emsley, P.; Lohkamp, B.; Scott, W. G.; Cowtan, K. Features and development of Coot. *Acta Crystallogr., Sect. D: Biol. Crystallogr.* **2010**, *66*, 486−501.
(47) Chen, V. B.; Arendall, W. B.; Headd, J. J.; Keedy, D. A.; Immormino, R. M.; Kapral, G. J.; Murray, L. W.; Richardson, J. S.; Richardson, D. C. MolProbity: all-atom structure validation for macromolecular crystallography. *Acta Crystallogr., Sect. D: Biol. Crystallogr.* **2010**, *66*, 12−21.
(48) Ethier, S. P.; Mahacek, M. L.; Gullick, W. J.; Frank, T. S.; Weber, B. L. Differential isolation of normal luminal mammary epithelial cells and breast cancer cells from primary and metastatic sites using selective media. *Cancer Res.* **1993**, *53*, 627−635.

DOI: 10.1021/acs.jmedchem.7b00193
J. Med. Chem. XXXX, XXX, XXX−XXX